# HUMAN VISUAL SYSTEM BASED FACIAL RECOGNITION FOR AUTONOMOUS SYSTEMS AND APPLICATIONS

A thesis submitted by

Qianwen Wan

In partial fulfillment of the requirements for the degree of

Master of Science

in

Electrical Engineering

Tufts University

May 2015



Adviser: Dr. Karen Panetta

## ABSTRACT

This thesis presents a real-time facial recognition system utilizing our human visual system algorithms coupled with classical Logical Binary Pattern (LBP) feature descriptors. Specifically, we first use the Weber's Law based human visual system to obtain decomposed images. Then, features are extracted using logarithmic Logical Binary Patterns (LBP). The contributions of this work include introducing region weighted models for facial components. We investigate two models, Hybrid region weighted model and Hybrid-Holistic region weighted model, and compare and contrast the performance on public databases of faces. Finally, the similarity ranking is obtained by fusing the chi-squared distance evaluated from each individual facial region. The system can quickly find and rank the closest matches of a test image to a database of stored images. For our prototype application, we supplied the system testing images and found their best matches in the database of training images.

This system can also be applied in many real life applications. One of them is automatically matching composite sketches to facial photographs. Different sketches hand drawn by artists or composite sketches synthesized using facial composite software can be compared to a database of photographs for the closest match. This is a particularly useful application for law enforcement agencies. Furthermore, other applications that could utilize this work include finding missing children or victims of human trafficking. Our methodology produces a low cost and efficient detection and recognition that weights more important facial features that may still be important to identify individuals, even though many years may have passed between the times the last known photograph

was taken. Often times, age progressed composite sketches are created to aid in the search. These sketches can be used in our system to help find individuals that have gone missing or to help locate wanted criminals.

Finally, we investigate the limitations of the system by applying the algorithms for other non-human facial features, namely matching animals. These experiments reveal the specialized features that researchers must take into consideration when searching for any subject possessing a “face”.

Experimental results have clearly shown the promising performance and a great value to law enforcement agencies.

## ACKNOWLEDGEMENT

I would like to thank Professor Karen Panetta for her guidance and advice throughout my whole graduate study. I also want to thank my friends in the Panetta Imaging and Simulation Laboratory and the Electrical and Computer Engineering department for their great company. Especially, Mr. George Preble.

Finally, I thank my father Qinzhong, mother Jijiao, and my grandmother Aifeng for encouraging and supporting me in my whole life.

## TABLE OF CONTENTS

## LIST OF TABLES

## LIST OF TABLES

# CHAPTER 1

# 1. INTRODUCTION

## 1.1. Facial recognition and Sketch recognition

A facial recognition system is a computer application for identifying or verifying a person from a digital image or a video frame from an imaging sensor such as a camera. Facial recognition has become one of the most popular areas of research in computer vision during the past several years. Facial recognition systems have produced successful applications for image analysis and understanding [1]. There are at least two reasons account for this trend: the first is the wide range of commercial and law enforcement applications, and the second is the availability of feasible technologies resulting from over 30 years of research [2].

Sketches are hand-drawn informal figures which are often created as a way of thinking about or working through a problem [3]. In many cases, we use sketches to match the most likely person, when the facial photograph of a person is not available.

A generalized procedure for the facial recognition problem can be presented as follows: Given still or video images of a scene, the process involves segmentation of faces from cluttered backgrounds, extraction of features from the facial region and then identify and match the person of interest using a stored database of faces. In order to narrow the search, available collateral information such as race, age and gender can be used. The generic face recognition task thus

posed is a central issue in problems such as an electronic line up and browsing through a database of faces [4].

### 1.2. Application for Facial recognition and Sketch recognition

Facial recognition systems are identification systems that use facial image processing. This area of research is becoming a very popular technology [5]. Facial image processing and analysis methods are most widely applied in identification and authentication. They have numerous applications in computer and physical access control, and digital entertainment[6]. Facial recognition technology (FRT) has numerous commercial and law enforcement applications. These applications range from static matching of controlled format photographs such as passports, credit cards, photo ID'S, driver's licenses, and mug shots to real-time matching of surveillance video images presenting different constraints in terms of processing requirements[4].

Helping to determine the identity of criminals is also an important application of facial recognition systems; however, in many cases the facial photograph of a suspect is not available. In these circumstances, drawing a sketch following the description provided by an eyewitness or the victim is a commonly used method to assist the police to identify possible suspects [7]. Due to budgetary reasons, many law enforcement agencies use facial composite software, which allows the user to create a computer generated facial composite (composite sketch), instead of employing forensic sketch artists [8].

Therefore, research on facial recognition and sketch recognition has become more significant and relevant in recent years owing to it potential applications [9]. Therefore, it is not surprising that it presents many challenging problems in the field of image analysis and computer vision[10].

### 1.3. Background work of Facial recognition and Sketch recognition system

Automated facial recognition has made dramatic progress over the past decade [11]. There are several related background concepts.

1) Image processing [12] : image processing is which the input is an image, such as a photo or video the output of image processing possibly will either be an image or a set of characteristics or parameters connected to the image. Image processing regularly refers to digital image processing, except optical and analog image processing also are likely.

2) Feature extraction [13]: When the input data to an algorithm is too large to be processed and it is suspected to be notoriously redundant, then the input data will be transformed into a reduced representation set of features. Transforming the input data into the set of features is called feature extraction. If the features extracted are carefully chosen, it is expected that the features set will extract the relevant information from the input data in order to perform the desired task using this reduced representation instead of the full size input.

3) Pattern recognition [14]: pattern recognition is the task of a label to a given input value. An illustration of pattern recognition is classification, which attempts to allot each input value to a particular group or bin. But, pattern recognition can encompass other types of output formats as well. Other illustrations are regression [12], which assigns a real-valued output to each input; succession labeling, which assigns a class to each member of a sequence of values and parsing, which assigns a parse tree to an input sentence, telling the syntactic structure of the sentence.

4) Facial recognition: A facial recognition system [15] is a computer application for systematically identifying or confirming a person from a digital image or a video frame from a video source. One of the behaviors to do this is by comparing selected facial features from the image to a facial database. It is classically used in security systems and can be compared to other biometrics such as fingerprint or eye iris recognition systems.

### 1.4. Challenging of current recognition system

#### 1.4.1. The image quality

The primary requirement of a facial recognition system is the expectation of the presence of good quality facial image as the input, which was collected under specified conditions. This could include lighting, pose and angle at which the photograph was obtained. The image quality is an important factor for extracting image features. The robustness of approaches will be lost if

the computation of facial features is not accurate. Thus, even the best recognition algorithms deteriorate as the quality of the image declines [16].

### 1.4.2. Illumination Problem

The same face may appear differently due to changes in lighting. Illumination can change the appearance of an object drastically. Robust systems must be able to perform quality image recognition in the presence of irregular lighting conditions [17].

### 1.4.3. Pose Variation

Since frontal facial images contain much more details of an individual, we usually use frontal images in testing prototype databases. However, the images captured by public access are rotated in daily life. The pose problem has been divided in to three categories: 1) Simple case with small rotation angle. 2) Most commonly addressed case, when there is a set of training image pairs, frontal and rotated images. 3)Most difficult case, when training image pairs are not available[18].

### 1.4.4. Facial expression

Facial expressions in particular are regarded as one of the most immediate and powerful means for humans to communicate their expressions, intentions and opinions to others. Therefore, facial expression plays an important role in the cognition of human expressions [19]. Face to face communication is largely based on implicit and nonverbal signals expressed through body, head

posture, hand gestures and facial expressions for determining the voice message unambiguously [20].

Facial expression is a unique and complicated aspect of humans. It is often difficult to express in few words what a single expression can communicate. Thus, this makes facial recognition even more challenging.

### 1.4.5. Other Challenges

Besides all those difficulties that are listed above, there are still plenty of challenges for real life facial recognition systems. Additional factors like aging (a natural biological change); plastic surgery (a medically induced change); non-permanent makeup; gender information to just name a few.

## 1.5. Thesis contribution and organization

This thesis presents a novel facial recognition approach which computes a description of weighted facial regions based on the combination of the properties of the Human Visual System (HVS) and Local Binary Patterns (LBP). The new system can evaluate the similarity between a training image and a testing image, as well as select a best matching image according to the similarity score.

A new composite sketch-to-photo facial recognition system is introduced where we demonstrate our new algorithms on public databases as well as our own sketch data base of Panetta Imaging

and Simulation Laboratory members for our experimental study. We synthesized composite sketches for each subject using a commercially available facial composite system, called Faces. We believe our prototype system will be of great value to law enforcement agencies.

In addition, we developed two different region weighted models based on single region contribution. The first one is called the hybrid region weighted model. The second model is called the holistic-hybrid region weighted model. By applying these two region weighted models, we improve the recognition results.

Furthermore, we utilize our recognition system to realize different real-life applications, such as finding missing children, tracking wanted criminals and finally test the limitations of our system for other non-human faces such as in pet-finding.

The remainder of this thesis is organized as follows:

Chapter 2 provides an overview of mathematical framework of the Human Visual System based image decomposition. Chapter 3 briefly reviews previously established Local Binary Pattern operators. Chapter 4 shows two different region weighted models. The effect of parameter selection on the algorithm is also presented. Chapter 5 presents a novel a real-time facial recognition system utilizing our human visual system algorithms coupled with logarithmic Logical Binary Pattern (LBP) feature descriptors. We perform our experiments using different public face databases. Chapter 6 proposes a new component-based sketch-to-photo recognition

system and lists several real-life applications. Finally, conclusions are drawn based on the experimental results of the presented materials.

A block diagram illustrating the flow of this thesis is shown in Figure 1.1

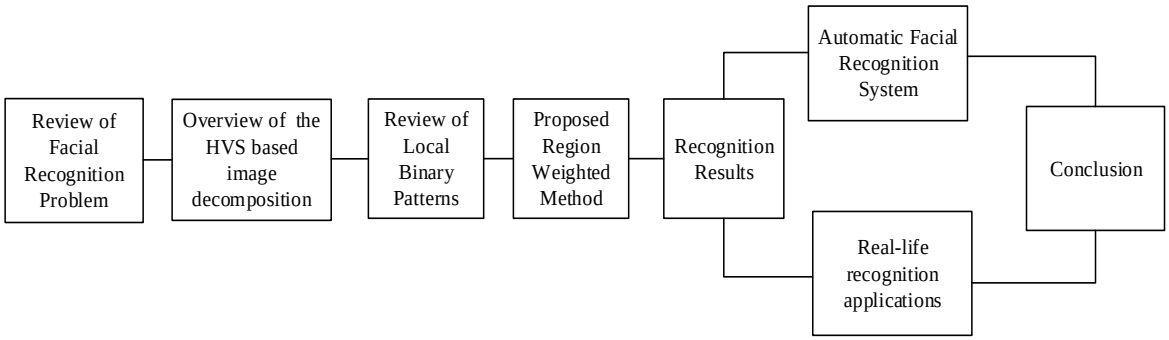


Figure 1.1 Flow diagram of the thesis

# CHAPTER 2

## 2. HUMAN VISUAL SYSTEM (HVS) BASED IMAGE DECOMPOSITION

Human Visual System (HVS) algorithms aim to provide a similar performance as human eyes, the best existing facial recognition machine, in a low-cost, accurate and efficient manner. Unlike other edge detection methods (Sobel [21, 22],Roberts [23],Prewitt[24],Canny[25, 26]), which are implemented in two steps: gradient image calculation and thresholding, the human visual system (HVS) is adapted to extract local structural information [27]. Common edge detection methods apply the same transform to all pixels in the image, regardless of local image information. However, in many cases, instead of using global algorithms, it is necessary to adapt the enhancement within local regions of the image. Therefore, the human visual system can be an effective method for using global algorithms locally in an image[28].

HVS algorithm is an excellent image processor capable of detecting and recognizing image information, it is only natural to bridge the gap between these psycho-physical attributes and the way in which images are represented and manipulated [29], [30], [31],[32]. Also, HVS is sensitive to relative, and not absolute, luminance changes for a large range of background intensities [33].

In this chapter, we will discuss human visual system based image decomposition, resulting in a more adaptive thresholding grayscale edge map, which more closely resembles how the human eye distinguishes objects from the background.

### 2.1. Human psychovisual phenomena[34]

The Human Visual System (HVS) based thresholding Algorithm is used for determining the most pertinent information and less informative data in an image. This is related to the human eye detect ability according to daily experience.

Brightness can be defined as the absolute brightness and relative brightness depends on the psychological sensation associated with the amount of light stimulus. Usually, absolute brightness could not be measured by the human eye because of its great adaptive ability. However, the relative brightness is an observer's feeling of difference in grayness between the objects. The term contrast is used to emphasize the difference in luminance of objects. The perceived grayness of a surface depends on its local background and the perceived contrast remains constant, if the ratios of contrasts between object and local background remain constant [35].

In psychology, contrast C refers to the ratio of difference in luminance of an object $B_o$ and its immediate surrounding $B_s$, i.e.

$$C = \frac{| B_o - B_s |}{B_s} = \frac{\Delta B}{B_s} \tag{2.1}$$

The visual increment threshold (or just noticeable difference) is defined as the amount of light necessary to add to a visual field of intensity B such that it can be discriminated from a reference field of the same intensity B. It therefore gives a limit for a perceivable change in luminance or intensity.

The major problems in a low intensity level image, which any image processing system has to deal with are[36]: (i) Detection of changes occurring in a low steady but visible illumination (i.e. minimum detectable change), and (ii) Detection of the mere presence or absence of light under a dark adapted condition (i.e. absolute visual threshold).

At a low intensity near the absolute visual threshold, the visual increment threshold $\Delta B_T$ is constant. With an increase in intensity $B$, $\Delta B_T$ converges symptomatically to the Weber behavior. This type of behavior is exhibited in a brightness incremental threshold for white broad band spectra and monochromatic narrow band spectra[37].

A characteristic response in the $\log \Delta B_T - \log B$ plane is presented in figure 2.1. There are four different types of regions of response characteristics displayed by the human eye. They are the De Vries-Rose region, the Weber region, the saturation region, and the dark region. The Weber behavior is characterized by the unit slope of the curve. The preceding region with slope 1/2 is known as the De Vries-Rose region. It has been shown [37] that if the central visual processor behaves as an optimum probabilistic detector, the incremental visual threshold follows the square root law, i.e. $\Delta B_T \propto \sqrt{B}$. However, in the actual case, this rule is followed in a small restricted

region (Figure 2.1). The dashed curve shows the deviation from Weber's law. This deviation, which represents a saturation region, is not usually exhibited by the retinal cone mechanism even under very high intensities, but could occur in very restricted cases.

From Figure 2.1 it is seen that variation of log $\Delta B$ against log$\Delta B$ in the De Vries-Rose region is slower than that in the Weber region. In other words, the discrimination ability in the De Vries-Rose region is greater than in the Weber region. The possible reason for this discrimination ability can be attributed to inherent visual nonlinearity.

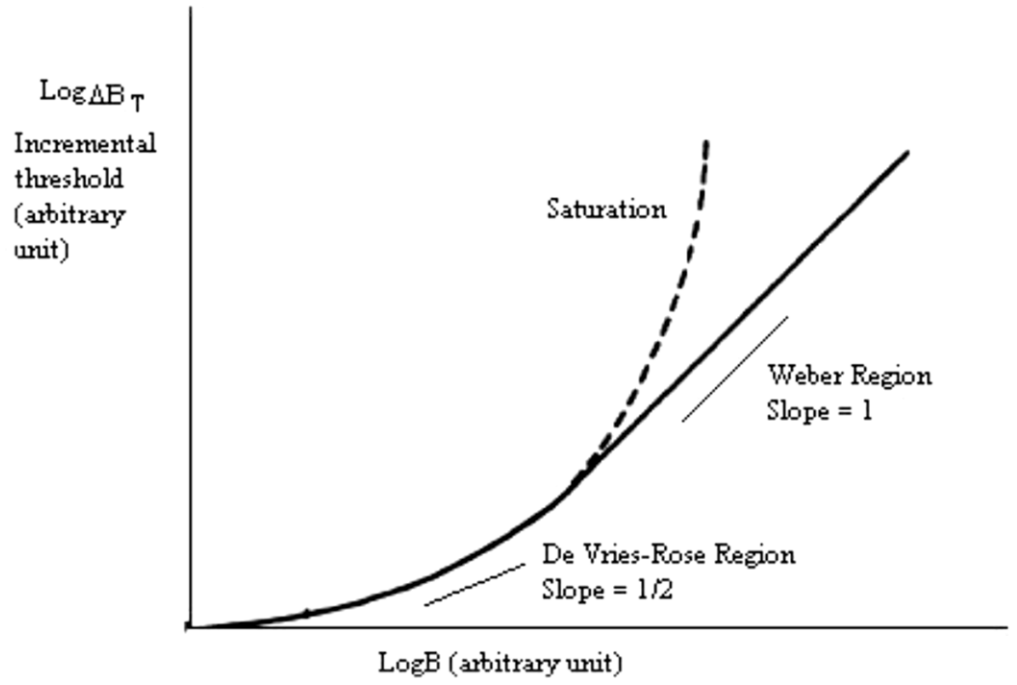


Figure 2.1: The increment threshold $\Delta B_T$ as a function of reference intensity B

According to Figure 2.1, the threshold values in the DeVries-Rose region, the Weber region and the saturation region are defined by the linear equations (2.2), (2.3) and (2.4) respectively:

$$\log \mathrm{B_T} = \log(\mathrm{K_1 B}) = \log \mathrm{B} + \log \mathrm{K_1} \quad (2.2)$$

$$\log B_T = \log\left(K_2\sqrt{B}\right) = \frac{1}{2} logB + logK_2 \quad (2.3)$$

$$\log B_T = 2logB + K_3 \quad (2.4)$$

## 2.2. Adaptive Thresholding [34]

As we know, adaptive thresholding is a thresholding method focusing on objects' location and environment brightness. All the thresholding details are described by the graph in Fig. 2.2.

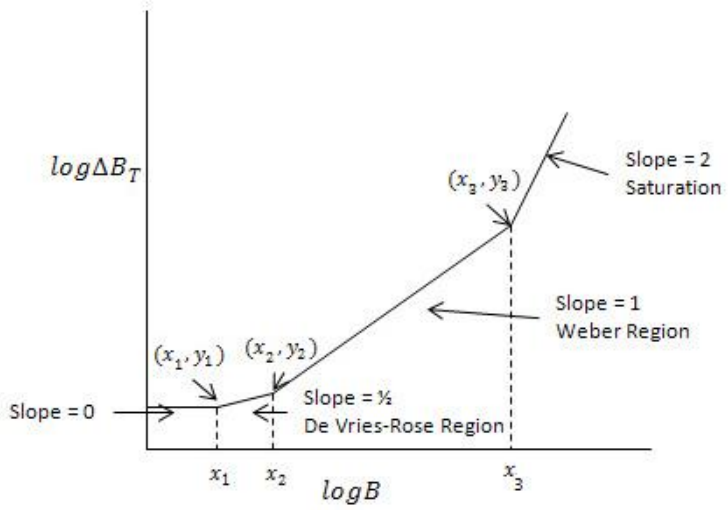


Figure 2.2: The Buchsbaum Curve: Approximation of the Increment Threshold log BT as a function of Reference Intensity log B.

In order to simplify the case and analysis we assume that the DeVries-Rose region extends between $x_1$ and $x_2$ (Figure 2.2) (x, corresponds to absolute visual threshold), the Weber region between $x_2$ and $x_3$ and the saturation region beyond $x_3$. The value of B corresponding to log B=$x_i$ is assumed here to be $B_x$, i=1, 2, 3. Hence,

$$x_i = logB_{x_i} \qquad for\ i = 1,2,3 \tag{2.5}$$

Let $X_o$ and $B_t$ be the maximum value of log B and B respectively. Let us assume further that

$$x_i = a_i x_0 \quad for\ i = 1,2,3 \tag{2.6}$$

$$B_{x_i} = a_i' B_t \quad for\ i = 1,2,3 \tag{2.7}$$

Where $0 < a_1 < a_2 < a_3 < 1,\ 0 < a_1' < a_2' < a_3' < 1$

The value of $\Delta B_T/B$ is remaining fairly constant over the entire Weber region with a value approximately equal to $\beta\,\%$ of the $(\frac{\Delta B_T}{B})_{\max}$, the maximum value over the entire dynamic range. Therefore, we can get,

$$K_1 = \frac{\Delta B_T}{B} = \frac{\beta}{100}(\frac{\Delta B_T}{B})_{max} \tag{2.8}$$

At the point (x2, y2), both (2.2) and (2.3) are satisfied according to Fig.2.2. Hence we can get,

$$y_2 = x_2 + logK_1 = \frac{1}{2}x_2 + logK_2 \tag{2.9}$$

Or,

$$\frac{1}{2}x_2 = \log(\frac{K_2}{K_1}) \tag{2.10}$$

Then from equation (2.6), we can get,

$$\frac{1}{2}logB_{x_2} = \log(\frac{K_2}{K_1}) \tag{2.11}$$

Or,

$$K_2 = K_1\sqrt{B_{x_2}} \tag{2.12}$$

Similarly, from the Fig 2.2 the point (x3, y3), we can get,

$$K_3 = K_1/B_{x_3} \tag{2.13}$$

The minimum values of the increment threshold corresponding to De Vries-Rose, Webber and Saturation regions are presented in (2.14),(2.15) and (2.16);

$$\Delta B_T = K_2\sqrt{B} = \frac{\sqrt{B}\beta}{100}\left(\frac{\Delta B_T}{B}\right)_{max}\sqrt{B_{x_2}},\ B_{x_2} \geq B \geq B_{x_1} \quad (2.14)$$

$$\Delta B_T = K_1\sqrt{B} = \frac{\sqrt{B}\beta}{100}\left(\frac{\Delta B_T}{B}\right)_{max},\ B_{x_3} \geq B \geq B_{x_2} \quad (2.15)$$

$$\Delta B_T = K_3\sqrt{B} = \frac{B^2\beta}{100}\left(\frac{\Delta B_T}{B}\right)_{max}\frac{1}{B_{x_3}}, B \geq B_{x_3} \quad (2.16)$$

Hence, for a particular pixel in an image having intensity Bp, we can have its thresholding formula given by:

Either, $\frac{\Delta B}{\sqrt{B}} \geq K_2\ when\ a_2'B_1 \geq B \geq a_1'B_1$ (2.17)

Or, $\frac{\Delta B}{B} \geq K_1\ when\ a_3'B_1 \geq B \geq a_2'B_1$ (2.18)

Or, $\frac{\Delta B}{B} \geq K_3\ when\ B \geq a_3'B_1$ (2.19)

With,

$$\Delta B = |Bp - B| \quad (2.20)$$

### 2.3. The Human Visual System based Thresholding Algorithm

In this section, we will use all the basic physical background knowledge to explain the HVS thresholding methods. By doing the thresholding process, we can produce the decomposed images according to the most pertinent information and less informative data in an image. Thresholding is based on the background intensity and the gradient information at each pixel. The background intensity can be calculated as a weighted local mean using the following formula (2.21):

$$B(x,y)=\frac{\frac{1}{2}\left(\frac{1}{4}\sum_{Q}X(i,j)+\frac{1}{4\sqrt{2}}\sum_{Q'}X(k,l)+X(x,y)\right)}{2} \tag{2.21}$$

Where B(x,y) is the background intensity at each pixel, X(x,y) is the input image, Q is all of the pixels which are directly up, down, left, and right from the pixel, and Q' is all of the pixels one pixel distance away in the diagonal directions. The gradient can be represented by any standard gradient detection algorithm. Here, we are using the Sobel operator. Thus the gradient is obtained using[38]:

$$G_x(x,y)=\begin{bmatrix}-1 & 0 & +1\\ -2 & 0 & +2\\ -1 & 0 & +1\end{bmatrix} * X(x,y) \tag{2.22}$$

$$G_y(x,y)=\begin{bmatrix}+1 & +2 & +1\\ 0 & 0 & 0\\ -1 & -2 & -1\end{bmatrix} * X(x,y) \tag{2.23}$$

$$X'(x,y)=\sqrt{G_x(x,y)^2+G_y(x,y)^2} \tag{2.24}$$

Here X'(x, y) is the gradient information and Gx ¸Gy are the directional gradients, while X(x, y) is the input image.

HVS also emulates the way human eyes respond to visual incentive. Information received by the human eye is characterized by attributes like brightness, edge information, and color shades. Brightness is actually a psychological sensation associated with the amount of light stimulus entering the eye [39]. Due to the adaptive ability of the human eyes, the eye cannot measure the

absolute brightness; rather eyes measure the relative brightness [34]. The maximum difference in the image can be obtained by (2.25):

$$B_T = \max(X(x,y)) - \min(X(x,y)) \tag{2.25}$$

Weber's Contrast Law quantifies the minimum change required for the human visual system to perceive contrast, however this only holds for a properly illuminated area. There are four different regions shown in the figure below, Devries–Rose Region is from x1 to x2, Weber Region is from x2 to x3, Saturation region is from x3 to infinity, and the fourth region is from the origin to x1, containing the least informative pixels. However, the minimum change required is a function of background illumination, and can be closely approximated with three regions, as shown in Fig.2.3 [40].

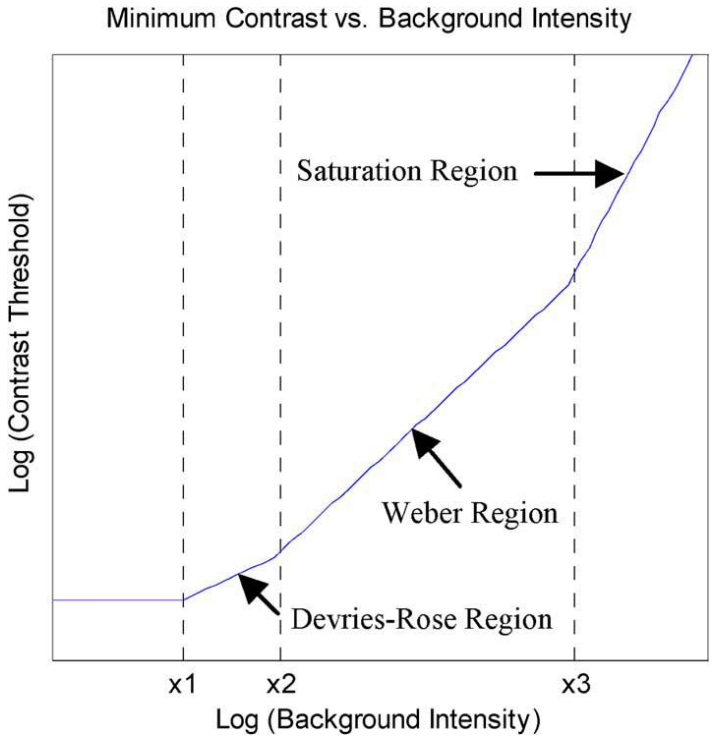


Figure 2.3 Four regions of human visual response

There are three different regions of response characteristics displayed by the human eye. The first one is De Vries-Rose region, which approximates this threshold for under-illuminated areas. The second region is the Weber region, which models this threshold for properly-illuminated areas. Finally, there is the saturation region, which approximates the threshold for over-illuminated areas.

The linear equations defining the De Vries-Rose region, the Weber region and the Saturation region are given respectively by,

$$\log \Delta B_T = \frac{1}{2} * \log B + \log K_2 \tag{2.26}$$

$$\log \Delta B_T = \log B + \log K_1 \tag{2.27}$$

$$\log \Delta B_T = 2 * \log B + K_3 \tag{2.28}$$

Here, K1, K2 and K3 are constants. The value of them is arrived at using the following formulas:

$$K_1 = \frac{1}{100} \beta * \max\left[ \frac{X'(x,y)}{B(x,y)} \right] \tag{2.29}$$

$$K_2 = K_1 \sqrt{B_{x2}} \tag{2.30}$$

$$K_3 = K_1 / B_{x3} \tag{2.31}$$

The thresholding parameter β in (2.29) determines the amount of information to be placed in the fourth region which is not defined in The Buchsbaum Curve. In this work, we set β as a constant 0.02. Then we assume Bxi corresponds to logB, for i = 1, 2, 3, so we can write:

$$B_{xi} = \alpha_i B_T \tag{2.32}$$

Where α1, α2, α3 are parameters based upon the three different regions of response characteristics displayed by the human eye. Since α1 is the lower saturation level, it is effective to set this to 0. For α2, α3, it is necessary to determine these experimentally. In [34] it was found that the best results occurred when these parameters were set to 0.1 and 0.9, respectively.

Using all this information, the image is first partitioned into the different regions of human visual response. These different regions are characterized by the formula for the minimum difference between two pixel intensities for the human visual system to register a difference. Next, these three regions are thresholded, removing the pixels which do not constitute a noticeable change for a human observer, placing these in a fourth image [41]. The formulas are:

$$\mathrm{Im}1 = X(x,y) \text{ for } B_{x2} \geq B(x,y) \geq B_{x1} \text{ and } \frac{X'(x,y)}{\sqrt{B(x,y)}} \geq K_1 \tag{2.33}$$

$$\mathrm{Im}2 = X(x,y) \text{ for } B_{x3} \geq B(x,y) \geq B_{x2} \text{ and } \frac{X'(x,y)}{\sqrt{B(x,y)}} \geq K_2 \tag{2.34}$$

$$\mathrm{Im}3 = X(x,y) \text{ for } B(x,y) \geq B_{x3} \text{ and } \frac{X'(x,y)}{\sqrt{B(x,y)}} \geq K_3 \tag{2.35}$$

$$\mathrm{Im}4 = X(x, y) \ \textit{for all remain pixels} \tag{2.36}$$

The thresholded images given by first three formulas in (2.33), (2.34) and (2.35) represent the regions where human eyes can perceive a noticeable difference in intensity with respect to the image background. The last one represents the regions in the image where the intensity values remain constant according to the human visual perception. So it is efficient to combine Im1, Im2 and Im3 for feature extracting. For our method, we use fusion methods to combine those useful regions together. In chapter 5, we will explain two different fusion methods in detail.

### 2.4. HVS Based Image Decomposition

HVS based image decomposition, which can segment the objects from their surroundings, provides a more accurate image pre-processing result.

1) In this stage, we first convert the input images into grayscale images.
2) Then we calculate the gradient magnitude and background information at each pixel of the grayscale images.
3) Finally, by referring to HVS based thresholding rules, we can decompose the images into sub-images, which are the Weber Region, the De Vries-Rose Region, the Saturation Region and remaining image pixels.

Fig. 2.4 is two examples of image decomposition results based on human visual system.

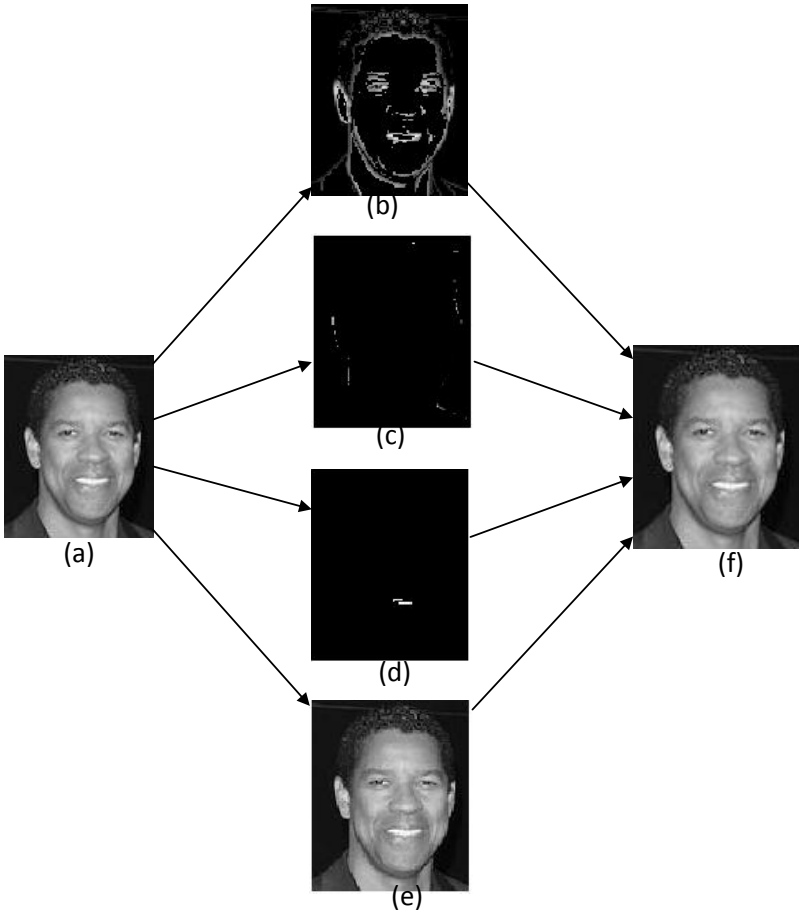


2.4(a) Original Grayscale Image (b) Weber Region (c) De Vries-Rose Region (d) Saturation region(e) Remaining image pixels (f) Result of addition fusion of (b), (c), (d)and(e)

## 2.5. Discussion about Parameter Selection for HVS

Two sets of parameters are used for image decomposition algorithms. They are the alpha parameter and the beta parameter. Changing the alpha and beta variants will produce a different dynamic thresholding algorithm. In this section of the thesis, we will discuss the effects obtained

by varying the alpha and beta parameters in the edge detection and image decomposition algorithms.

### a. Alpha variation

The alpha parameters determine the boundary of the different regions for HVS based image decomposition. The selection of alpha values depends on how much weight needs to be placed on the individual regions. The Weber region is given the maximum weight because it contains most of the illumination changes compared to the other regions in the HVS based image decomposition. The typical values chosen for alpha parameters are: $\alpha 1 = 0,\ \alpha 3 = 0.1$ and $\alpha 2 = 0.9$ for image decomposition.

### b. Beta variation

Beta is the thresholding parameter for HVS based image processing algorithms. A very low value of beta may result in false edges appearing in the edge map. Increasing the value of beta to a great extent may result in loss of edges. The value of beta also depends on the choice of the image. Here is a table that lists the selections of different beta value [42].

Table 2.1 Summary of beta values[42]

| Range of beta | Typical Values | Applications |
|---|---|---|
| Low | 0.001 – 0.005 | Edge detection in synthetic images |
| Medium | 0.02 – 0.06 | Edge detection in natural images, edge based feature |

| | | |
|---|---|---|
| | | extraction from natural images and other applications involving the gradient image. |
| High | 0.2-0.4 | Amount of gradient information to be retained is really low. |

### 2.5.1. Image edge detection based on HVS

In the section, we will show some examples of edge detection based on Human Visual System. As stated above, the essence of HVS based edge detection is to decompose the image into four different regions based on local information and background intensity and then apply an adaptive threshold on it. Then, we can get a grayscale edge map which keeps the most important information of an image.

### 2.5.2. Experimental binary results of different kinds of edge detection

In this section, we present a comparison between a HVS based edge map and other common edge detection methods. In order to realize a binary edge map, we select a threshold value manually.

| | |
|---|---|
|  (a) |  (b) |
|  (c) |  (d) |
|  (e) |  (f) |

(g)

(h)

Figure 2.5(a) Original Image, (b) Original Grayscale Image , edge detection binary results using(c) Roberts, (d) Sobel, (e) LoG edge detection, (f) Prewitt, (g) Canny, (h) HVS based edge detection

Here, we will use a non-reference edge measurement to compare all the edge maps listed above. The established Non-reference Reconstruction based Edge Measure (NREM) is developed by Karen Panetta and Chen Gao[43]. And the results listed in table 2.2 are base on the binary edge maps in Fig.2.5. The bigger value means better binary edge map.

Table 2.2 Example NREM comparison result

| Edge Measure | Roberts | Sobel | LoG | Prewitt | Canny | **HVS** |
|---|---|---|---|---|---|---|
| NREM value | 0.3918 | 0.6513 | 0.3645 | 0.6897 | 0.1318 | **0.7607** |

## 2.6. Experimental Results of grayscale edge map of HVS based edge detection

| Original Image | Grayscale edge map |
|---|---|
|  |  |
|  |  |
|  |  |

| | |
|---|---|
|  |  |
|  |  |
|  |  |

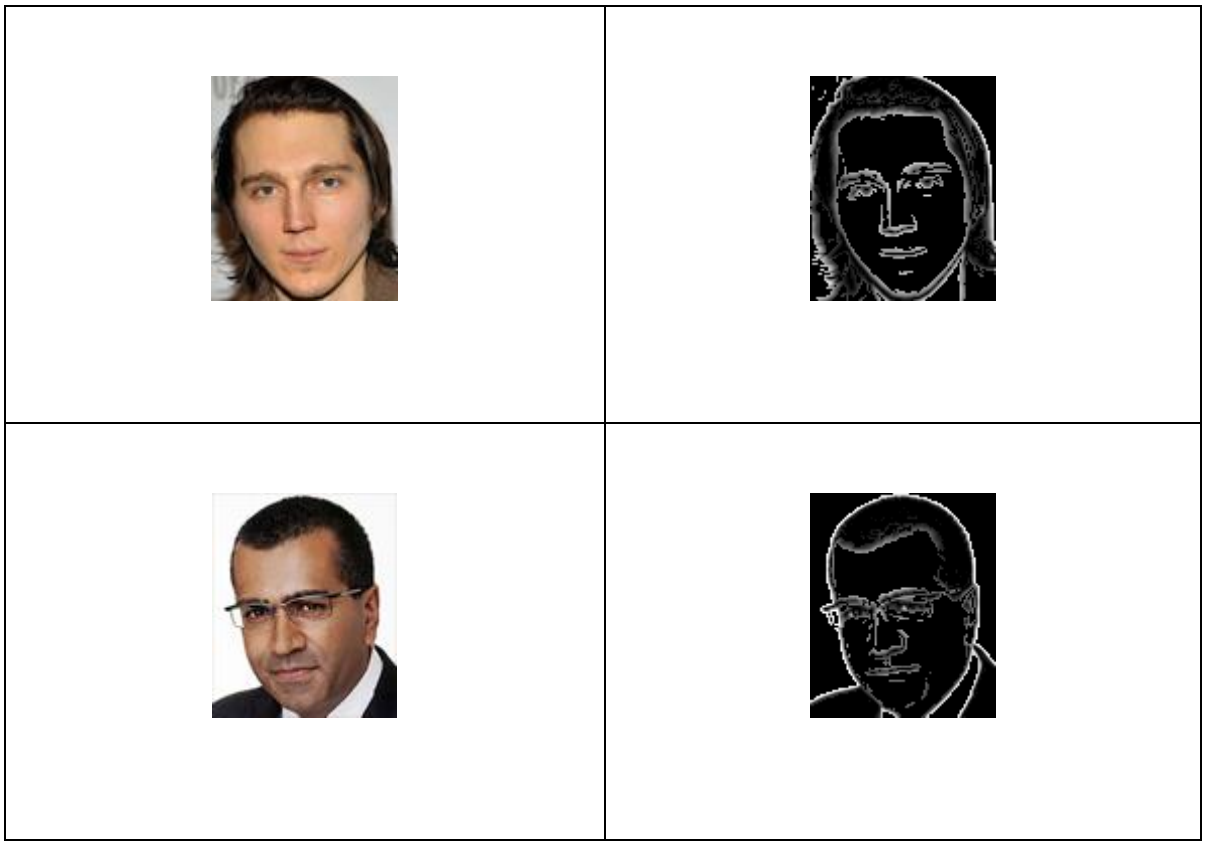

Figure 2.6 the pictures of left row are original images and the pictures of right row are grayscale edge map using HVS based edge detection

# CHAPTER 3

## 3. A REVIEW OF LOCAL BINARY PATTERN FOR FACIAL RECOGNITION

Facial recognition involves two crucial aspects: facial feature representation and classifier design [44]. Facial feature representation is a fundamental step for facial recognition, which means that if we cannot extract enough feature information or we capture too much useless information, even the best classifier design will fail. Hence, it is very important to create a good facial feature representation.

Normally, there are three basic principles for a "Good" facial feature representation. First of all, the feature representation can tolerate the within-class variations whilst discriminate different classes well. Second, it can be easily and quickly extracted from the raw images. Last, it lies in a space with the low dimensionality in order to avoid computationally expensive classifiers [44].

There are many existing algorithms for describing facial features: Principal Component Analysis (PCA) [45], Linear Discriminate Analysis (LDA) [46], and Independent Component Analysis (ICA) [47] have been widely introduced for feature extraction, and recently, representations based on the outputs of Gabor filters [48] at multiple scales, orientations, and locations have achieved superior performance for facial image analysis in [49] and [50].

Local Binary Patterns (LBP) [51], a non-parametric method summarizing the local structures of an image efficiently, has received increasing interest for facial representation recently [52], [53].

Tolerance against the monotonic illumination changes and computational simplicity is its biggest advantage.

Up to now, Local Binary Patterns features have been extensively exploited for facial image analysis, including face detection [54], [55], [56], face recognition [52], [57], [58], [59], [60], [61], [62], facial expression analysis [63], [64], [65], [66], gender and age classification [67], [68], and some other applications [69], [70]. LBP was originally proposed for texture description[71], and has been widely exploited in many applications such as image and video retrieval, aerial image analysis, and visual inspection.

In this chapter, we will review different LBP methodologies in context of facial image analysis.

### 3.1. Classical Local Binary Patterns

A local binary pattern (LBP) is a type of feature used for classification in computer vision. LBP is the particular case of the Texture Spectrum model proposed in 1990. LBP was first described in 1994[72]. It has since been found to be a powerful feature for texture classification; it has further been determined that when LBP is combined with the Histogram of oriented gradients (HOG) descriptor, it improves the detection performance considerably on some datasets [13]. In this section, we will review the basic idea and concept of classical Local Binary Patterns.

The original LBP operator focused on every pixel of an image by thresholding a 3x3 neighborhood window. Then, the next step is labeling according to the center pixel value. When

the center pixel's value is greater than the neighbor's value, write "1". Otherwise, write "0". By doing this we will get an 8-digit binary number (which is usually converted to decimal for convenience).

Fig.3.1 is a specific example using to demonstrate the LBP operator. The derived binary numbers are called Local Binary Patterns or LBP codes.

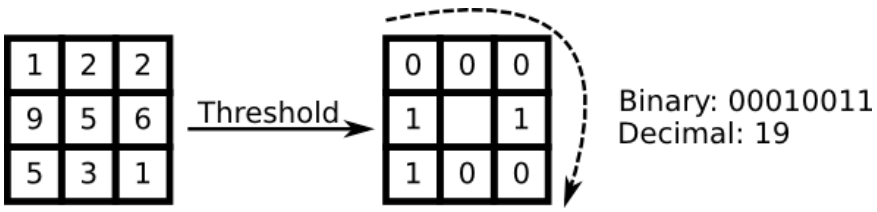


Figure 3.1 An example of the basic LBP operator

At a pixel ($x_c$, $y_c$), the resulting LBP can be expressed in [73]:

$$LBP(x_c, y_c) = \sum s(i_n - i_c)2^n \tag{3.1}$$

Where, $i_n$ and $i_c$ are gray-level values of the central pixel and the surrounding pixels, and the function s(x) is defined as:

$$s(x) = \begin{cases} 1 & if\ x \geq 0 \\ 0 & if\ x < 0 \end{cases} \tag{3.2}$$

Since a small 3x3 LBP neighborhood cannot capture the dominant features with large scale structures, the operator was later considered to use neighborhoods of different sizes[51]. The basic LBP method uses a notation (P, R) to present a small circularly symmetric neighborhood which has P equally spaced pixels on a circle of radius R.

Fig. 3.2 shows some variants of circular neighborhood.

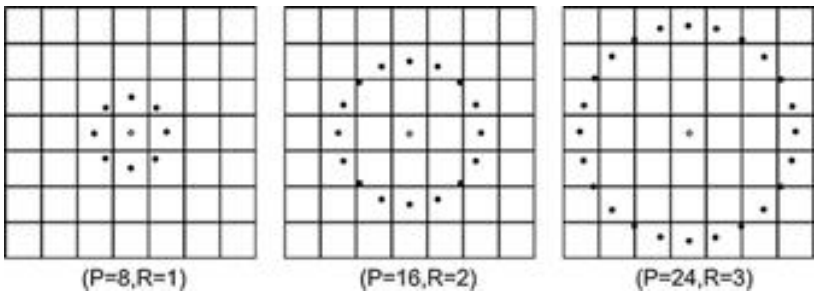


Figure 3.2Examples of the extended LBP operator[52]: From left to right are the circular (8, 1), (16,2),and (8, 2) neighborhoods

### 3.2. Uniform Local Binary Patterns

Based on the explanation in 3.1, the LBP operator LBP (P, R) can produce $2^p$ different output values. It has been shown that some patterns contain more information than the others[52] among these $2^p$ different binary patterns formed by the P pixels in the neighborhood. However, people find that using only a subset of the $2^p$ binary patterns to describe the texture of the images can simplify the computation and analysis.

An extension to the original operator uses uniform patterns [51]. A local binary pattern is called uniform if the binary pattern contains at most two bitwise transitions from 0 to 1 or vice versa when the bit pattern is considered circular. For example, the patterns 00000000 (0 transitions), 01110000 (2 transitions) and 11001111 (2 transitions) are uniform whereas the patterns 11001001 (4 transitions) and 01010011 (6 transitions) are not. In the uniform LBP mapping,

there is a separate output label for each uniform pattern, and all the non-uniform patterns are assigned to a single label. For instance, the uniform mapping produces 59 output labels for neighborhoods of 8 sampling points. Using uniform patterns instead of all the possible patterns has produced better recognition results in many applications. It also enables significant space savings when building LBP histograms.

Moreover, the uniform patterns create a visualization of the LBP method as a unifying approach to the traditionally divergent statistical and structural models of texture analysis [52]. Each pixel is labeled with the code of the texture primitive that best matches the local neighborhood. Thus each LBP code can be regarded as a micro-Textron [74]. Local primitives detected by the LBP include spots, flat areas, edges, edge ends, curves, and so on. Some examples are shown in Figure 3.3 with the LBP 8,R operator. In the figure, ones are represented as black circles, and zeros are white.

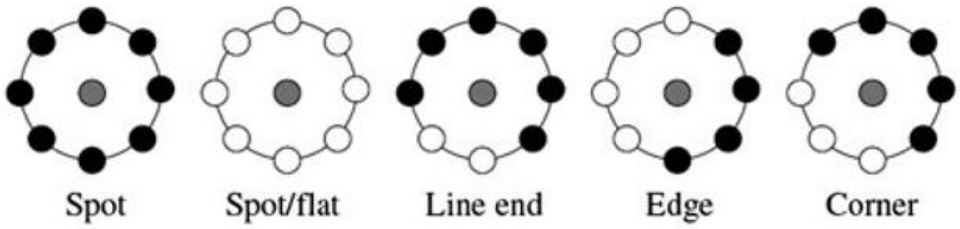


Figure 3.3 Different texture primitives detected by the LBP

Ojala et al. noticed that in their experiments with texture images, uniform patterns account for a bit less than 90% of all patterns when using the (8, 1) neighborhood and for around 70% in the (16, 2) neighborhood. Especially in experiments with facial images, it was found that 90.6% of

the patterns in the (8, 1) neighborhood and 85.2% of the patterns in the (8, 2) neighborhood are uniform [74] . According to the analysis above, we can choose to apply the Uniform LBP for three outstanding advantages: universality, statistical robustness, and efficiency.

### 3.3. Improved Local Binary Patterns

Jin et al. [54] pointed out that LBP could miss the local structure information under some circumstances. So they developed the ILBP (Improved Local Binary Patterns).

Instead of comparing with only the central pixel, the ILBP method compares all the pixels (including central pixel) with the mean value of the neighborhood in the kernel (as shown in Fig. 3.4). Later ILBP was extended to the neighborhoods of any sizes. By doing this, we can get a more complete information.

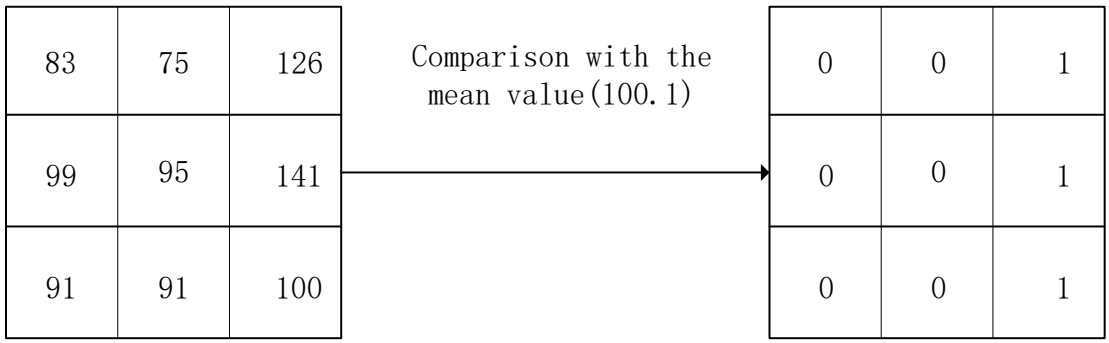


Figure 3.4 An example of the ILBP

### 3.4. Extended Local Binary Patterns

There are two common types of Extended Local Binary Pattern. One of them is proposed by Huang et al [75]. They state that the classical Local Binary Patterns and Uniform LBP can only reflect the first derivation information of the facial image instead of presenting the velocity of local variation, which is useful information to describe the local appearance patterns. In order to solve this problem, they extended LBP to encode the derivative image.

Since an image is a function of multiple variables, they take the horizontal and the vertical directions. Using $h_x$ to denote a horizontal derivative filter (matrix), $h_y$ to denote a vertical derivative filter (matrix), two descriptions are considered: Gradient magnitude and Gradient direction.

$$|\nabla I| = \sqrt{(h_x \otimes I)^2 + (h_y \otimes I)^2} \tag{3.3}$$

And

$$\phi(\nabla I) = \arctan\left(\frac{h_y \otimes I}{h_x \otimes I}\right) \tag{3.4}$$

Sobel filtering is used for generating two derivative images, and then the gradient magnitude images are produced. This method applies LBP operators to both original image and gradient magnitude image.

Another Extended LBP (ELBP) was proposed in [76], which is similar to 3DLBP. The ELBP operator not only indicates binary comparisons between the central pixel and its neighbors, but

also encodes the exact gray-level value differences (GD) between them by adding several binary units.

### 3.5. Advanced Local Binary Patterns

Liao et al.[64]proposed Advanced LBP (ALBP) [64], it is used to exploit rotation invariant LBP for facial expression recognition.

For ALBP (Advanced Local Binary Pattern), each pattern in the image is assigned a unique label by the equation below:

$$\mathrm{LBP}(m, R) = \sum_{i=0}^{p-1} u(t_i - t_c)2^i \quad (3.5)$$

Where $t_c$ is the intensity of the central pixel in a neighborhood, $t_i$ is the intensity of the neighborhood pixel i, and u(x) is the step function. Therefore, the ALBP pattern group is defined as:

$$\mathrm{ALBP}^g(m, R) = \min\left(\mathrm{Cir}(\mathrm{LBP}(m, R), n)\right) \quad (3.6)$$

Where n = 0, 1... p- 1, Cir(x, n) performs a circular anti-clockwise bitwise shift on the p-bit number by n times.

In their study, the ALBP histogram was sorted in a descending order, and the first several entries in the histogram were treated as the dominant patterns. Their results show that nearly 80% of these patterns are quite sufficient for representing faces[64].

### 3.6. Modified Local Binary Patterns

The Human face is a near-regular texture pattern generated by facial components and their configurations. Considering facial components such as eyebrow, eye, pupil, nose and face boundary, in paper [77] they select 8 main different spatial templates shown in Fig. 3.5 to preserve shape information of facial components.

With only those spatial templates, all facial components are described; for example, eyebrow can be described by a union of templates $P_4$, $P_3$ and $P_2$. They combine all those spatial and local texture information to improve the capacity of describing faces.

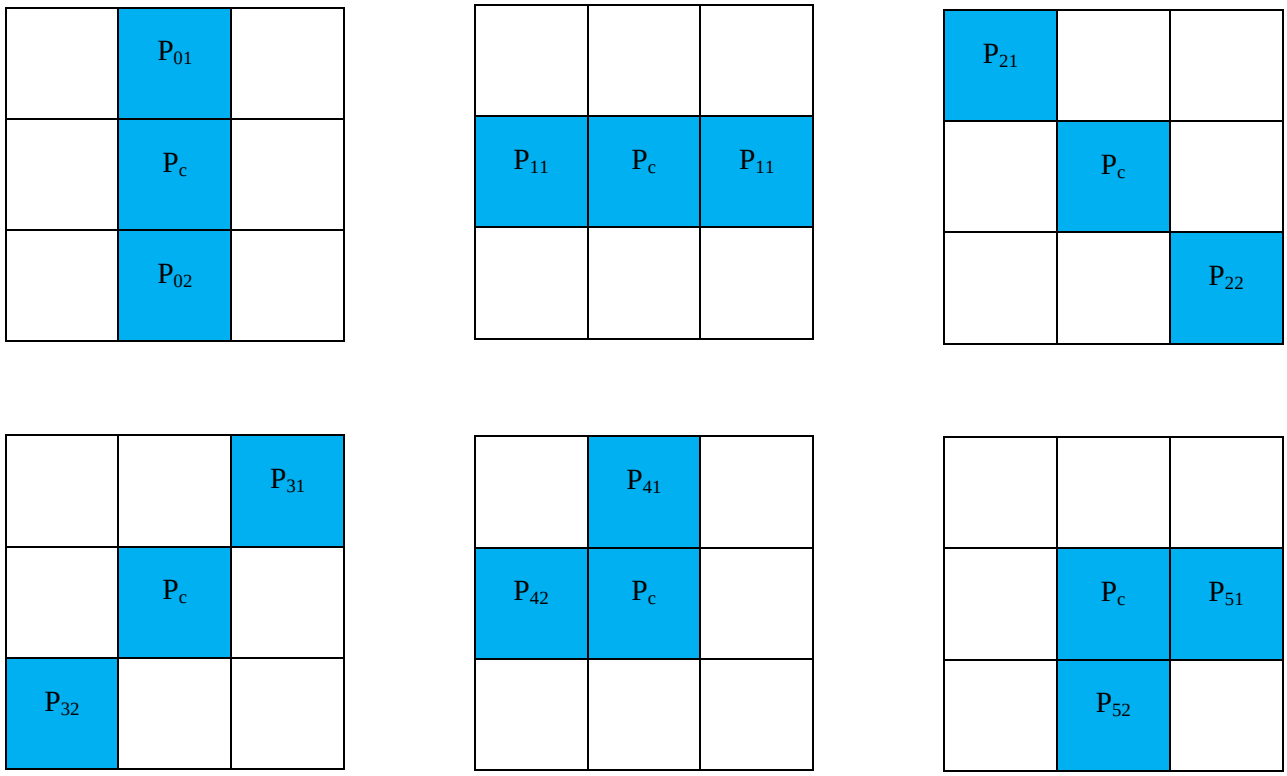

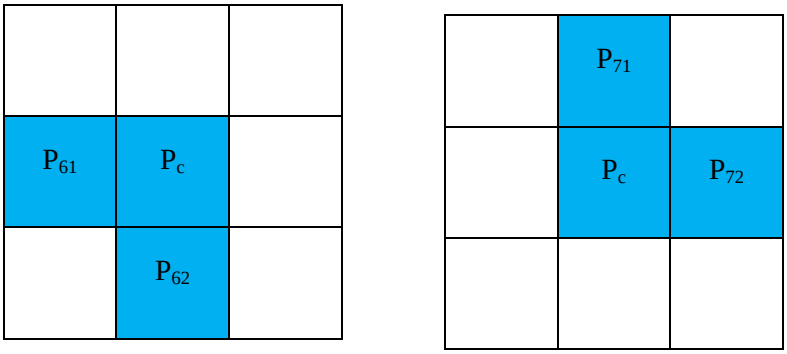


Figure 3.5 Eight main spatial templates

In their method, they use each pair of two neighborhood pixels ($P_{i1}$, $P_{i2}$) according to spatial templates to compare with the central pixel Pc. Eight spatial templates form 8 binary digits of MLBP number. So MLBP operator produces 256 different values. Equation below gives the computation of MLBP number.

$$MLBP = \sum_{l=0}^{7} Si(x) \times 2^{i} \tag{3.7}$$

Where $S_i$ is the $i^{th}$ binary digit of MLBP number;

$$Si(x) = \begin{cases} 1, (Pc > P_{i1}) and (Pc > P_{i2}) \\ 0, \quad otherwise \end{cases} \tag{3.8}$$

Using this method, we can retrieve more information to distinguish face and non-face objects.

### 3.7. Hamming Local Binary Patterns

Yang and Wang [78] proposed a Local Binary Patterns method to deal with facial images containing noise. They observed that, for facial regions, especially the ones with noise, the non-uniform patterns account for a much larger percentage compared with uniform patterns in their experiments. They proposed to reclassify the non-uniform patterns based on the Hamming distance, instead of accumulating them into a single bin as LBPu2 do.

In the Hamming LBP, the non-uniform patterns are incorporated into the existing uniform patterns by minimizing Hamming distance between them. For example, non-uniform pattern $(10001110)_2$ is converted into uniform one $(10001111)_2$ since their Hamming distance is one. In case several uniform patterns have the same Hamming distance with a non-uniform pattern, the one with minimum Euclidian distance is chosen. Experimental results illustrate that Hamming LBP is a proper enhancement for face recognition [78].

### 3.8. Local Ternary Patterns

Tan and Triggs [58] argued that the original LBP tends to be sensitive to noise, especially in near-uniform image regions, because it thresholds exactly at the value of the central pixel. Therefore, they extended the original LBP to a version with 3-valued codes, called Local Ternary Patterns (LTP). In LTP, the indicator s(x) in (1) is replaced by:

$$s'(i_n, i_{c,} t) = \begin{cases} 1, & i_n > i_c + t \\ 0, & |i_n + i_{c|} < t \\ 1, & i_n \leq i_c - t \end{cases} \quad (3.9)$$

Where t is a user-specified threshold. The LTP codes are more resistant to noises, but no longer strictly invariant to gray-level transformations. The experimental results show that LTP provides better performance than LBP for face recognition under the difficult lighting conditions. In [66], LTP and LBP achieved similar results for facial expression recognition.

### 3.9. Elongated LBP

The main reason to define the neighborhood on a circle in the original LBP is to resolve the rotation invariant problem for texture description. However, Liao and Chung [59]argued that, in the applications like facial image analysis, the rotation invariant problem does not exist; instead, the anisotropic information is treated as important features. Therefore, they proposed the Elongated LBP with neighboring pixels lying on an ellipse.

Different from building a neighborhood on a circle, they proposed the Elongated LBP with neighboring pixels lying on an ellipse. Fig.3.6 gives two examples of the Elongated LBP, where A, B denote the long axis and the short axis respectively, and m is the number of the neighboring pixels. The coordinate ($g_{ix}$, $g_{iy}$) of each neighboring pixel $g_i$ (i = 1, 2..., m) with respect to the central pixel is defined as:

$$g_{ix} = R_i * cos\theta_i, g_{iy} = R_i * sin\theta_i \quad (3.10)$$

$$R_i = \sqrt{\frac{A^2B^2}{A^2sin^2\theta_i + B^2cos^2\theta_i}} \tag{3.11}$$

$$\theta_i = (\frac{360}{m} * (i-1))^\circ \tag{3.12}$$

The Elongated LBP operator could be rotated along the central pixel with a specific angle to characterize the elongated structures in different orientations, achieving multi-orientation analysis in face images. The experimental results demonstrate that the Elongated LBP outperforms the original LBP for face recognition tasks[59].

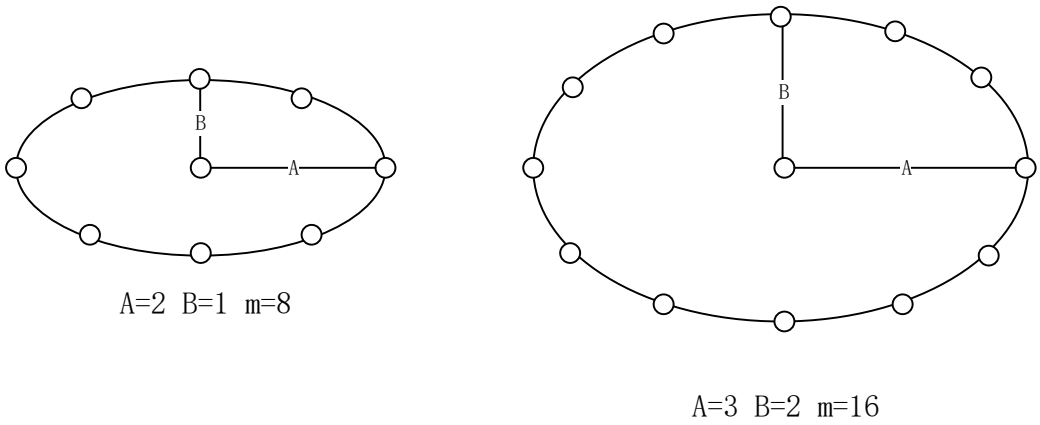


Figure 3.6 Two examples of the Elongated LBP

Zhao and Pietikäinen [65], [79]extended the original LBP to Volume LBP (VLBP), also called 3D-LBP, to describe dynamic texture. For each pixel, neighboring pixels in the volume are compared with the central pixel to obtain the binary units, for which the weights are given according to a spiral line. In order to make VLBP computationally simple and easy to extend,

only co-occurrences on the Three Orthogonal Planes are considered, resulting a simpler version, named LBP-TOP.

As shown in Fig. 3.7, the dynamic texture is modeled with the concatenated LBP histograms from these three orthogonal planes. The traditional circular sampling is replaced by an elliptical sampling so that different radiuses are set in space and time domain. The VLBP and LBP-TOP have been successfully used for dynamic texture recognition [79] and facial expression recognition [65, 79]. One drawback of this extension is the high dimensionality of the feature vector.

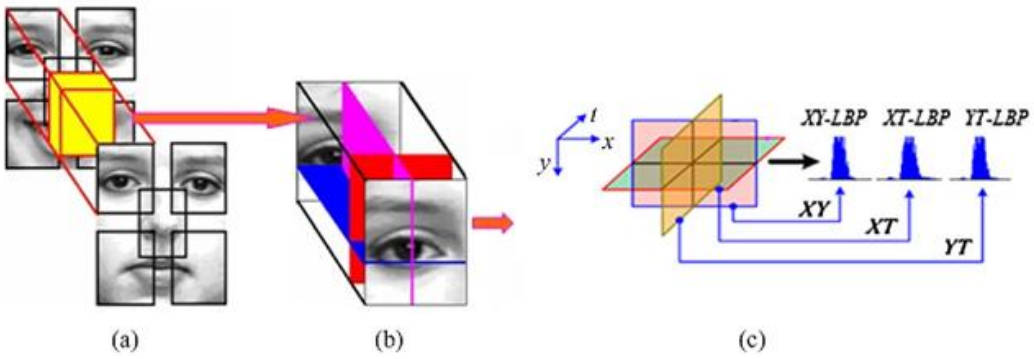


Figure 3.7 VLBP features in each block volume[79]

Fu and Wei[80] introduced the Centralized Binary Patterns (CBP) for facial expression recognition. As illustrated in Fig. 3.8, CBP compares pairs of neighbors which are in the same diameter of the circle, and also compares the central pixel with the mean of all the pixels (including the central pixel and the neighboring pixels), given the largest weight to strengthen the effect of the central pixel. Compared to the original LBP, CBP produces less binary units,

and thus reducing the feature vector length. For example, $CBP_{(8,1)}$ shown in Figure. 3.8 outputs five binary units (s($g_0 - g_4$), s($g_1 - g_5$), s($g_2 - g_6$), s($g_3 - g_7$), s($g_c - g_T$)), while $LBP_{(8,1)}$ produces eight binary units. CBP was shown to be superior to original LBP for facial expression recognition.

$$\mathbf{CBP}_{(8,1)} = \mathbf{s(g_0 - g_4)2^0 + s(g_1 - g_5)2^1 +}$$

$$\mathbf{s(g_2 - g_6)2^2 + s(g_3 - g_7)2^3 + s(g_c - g_T)2^4};$$

$$\mathbf{g_T = (g_0 + g_1 + \cdots + g_7 + g_c)/9}$$

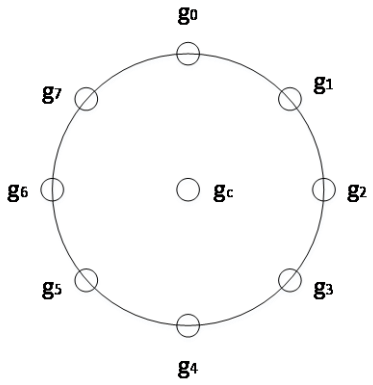


Figure 3.8 An example of CBP

### 3.10. Logarithmic LBP

In [81], Debashree Mandala, Karen Panetta, and Sos Agaian introduced Logarithmic-LBP operators. In this approach instead of using the raw image pixels, a logarithmic transform is applied on the image and the then the LBP features are extracted in the logarithmic domain.

Let $f(x,y)$be the input image then the image in the logarithmic domain is given by:

$$I(x,y) = log\left[eps + \left(\frac{f(x,y)}{\max(f(x,y))}\right)^{\alpha}.f(x,y)\right] \quad (3.13)$$

Where $\alpha$ is the parameter. In our experiments they have used several values of this parameter and obtained the results. The LBP feature extractor is then applied in the logarithmic domain to extract the LBP feature vectors. Uniform LBPs are used for face recognition as they outperform the other variants of LBP available. Here is a small number to avoid error in presence of zero image intensities. They have used feature fusion where the histograms generated from different values of the parameter alpha are concatenated to obtain an improvement in the average rate of recognition.

Computer simulations have shown using logarithmic LBP operators can improve the rate of recognition using the AT&T Laboratories face database. [81]

### 3.11. Comparison of Local Binary Patterns

This section presents a comparison on the Local Binary Patterns (LBPs) for facial recognition and its many variants. Here is a list of comparison of LBP variations.

Table 3.1 comparison of current Local Binary Pattern

| LBP variations | Properties | Advantages |
|---|---|---|
| Uniform LBP | The uniform mapping produces 59 output labels for neighborhoods of 8 sampling points. | Universality, statistical robustness, and efficiency. |

| | | |
|---|---|---|
| Improved Local Binary Patterns | Consider effects of center pixels | Enhances discriminative capability |
| Extended Local Binary Patterns | Consider effects of derivative image. | Enhances discriminative capability |
| Advanced Local Binary Patterns | Consider effects of rotation of facial images | Enhances discriminative capability for facial expression. |
| Modified Local Binary Patterns | Considering facial components such as eyebrow, eye, pupil, nose and face boundary | Retrieves more information to distinguish face and non-face objects. |
| Hamming Local Binary Patterns | Incorporate non-uniform Patterns into the uniform patterns | Enhances discriminative capability |
| Local Ternary Patterns | Bring in new thresholds | Improves the robustness, especially for noise image. |
| Elongated LBP | Not invariant to rotation | Capable to choose different Neighborhood and consider rotation as a texture |
| Volume LBP | Describe dynamic texture | Extending to 3D facial image |
| Centralized Binary Patterns | Give the largest weight to strengthen the effect of the central pixel | Produces less binary units, and thus reducing the feature vector length, good for facial expression recognize. |
| Logarithmic LBP | Pre-process the images in logarithm domain | Enhances discriminative capability |

Based on the comparison results, we choose Logarithmic Local Binary Patterns to extract images features.

### 3.12. Experimental results of logarithmic LBP process

Here, we will present the results for logarithmic LBP process. First, we apply the HVS based image decomposition for the grayscale image, and then transfer the result into logarithmic domain. Finally, we will get the logarithm LBP feature vectors.

| Original image | HVS based image decomposition | HVS based image after logarithmic transform | Extracted logarithm LBP feature vector |
|---|---|---|---|
|  |  |  | 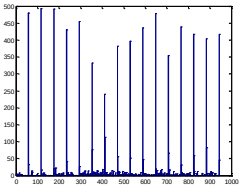 |

| | | | |
|---|---|---|---|
|  |  |  | 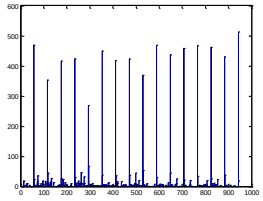 |
|  |  |  | 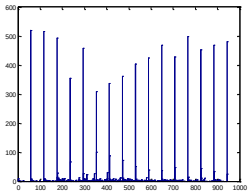 |
|  |  |  | 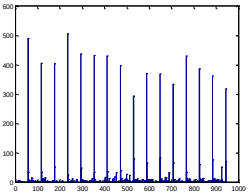 |
|  |  |  | 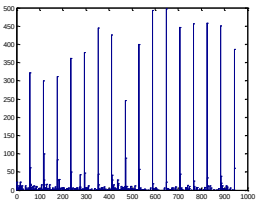 |

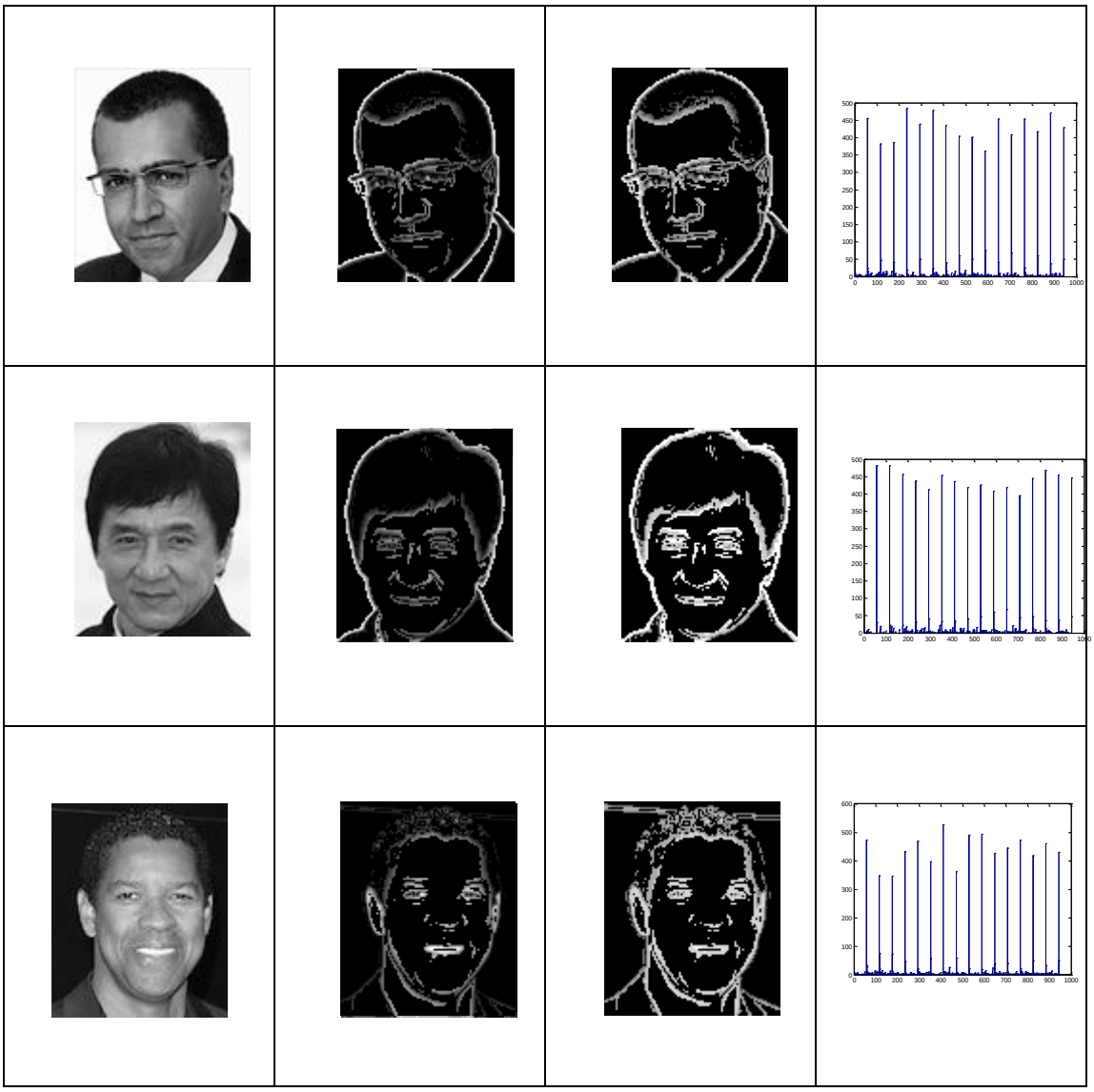

Figure 3.9 Example Logarithm LBP process results

# CHAPTER 4

## 4. REGION WEIGHTED MODEL FOR FACIAL RECOGNITION USING FACIAL COMPONENTS

While there have been tremendous improvements for automatic facial recognition systems, there is still much more work to be done to improve current methods to match the performance and accuracy of the human evaluator for facial recognition. In Harandi's work [82] two reasons are provided that summarize the issues of the current methods:

1) Most current approaches for Automatic Facial Recognition systems attempt to use the same engineering solutions used for general object recognition where the target object of interest is non-human. However, recognizing human faces is a special task that varies across the regions of the face and should not be treated as a single object.

2) Facial recognition involves analyzing information about individual facial features (mouth, nose, eyes, etc.), but also requires processing information about the spatial layout or configuration of facial features (holistic view) [83].

Based on the psychophysical findings, there is no doubt that some facial features (such as eyes, nose and mouth) play more important roles in human facial recognition applications than other features[84]. In this section, we will propose two different region weighted methods based on the contribution of the most distinctive facial features.

The first one is called Hybrid Region Weighted model. Instead of striving for a holistic description, the first model utilizes a hybrid approach, which weights the contribution of distinctive facial features.

The second model is called Holistic-Hybrid Region Weighted model. According to the second principle above, it is generally agreed that faces are not recognized only by utilizing some holistic search, but also through a feature analysis that is aimed at specifying more important features of each specific face. Hence this method uses both holistic and facial component (eye, nose and mouth) feature analysis to recognize faces.

### 4.1. Motivation of Region Weighted Model for Facial Recognition

A fundamental challenge in facial recognition lies in determining which facial characteristics are important in the identification of faces. Therefore weighting the contribution of the distinctive facial features is useful for a successful facial recognition system.

In the real life, people recognize faces of their own race more accurately than faces of other races. The "contact" hypothesis suggests that this "other-race effect" occurs as a result of the greater experience we have with our own race versus other-race faces [85]. Levin hypothesized that when people see cross-racial faces, they code race-specifying information at the expense of individual information, something they don't do when they see racial faces that match their own race. For instance, Caucasian and Non-Caucasian people have different opinions about facial feature capturing with Asian people. Several studies have shown that, Asian people tend to pay

more attention on eyes and noses when they recognize faces, while Caucasian people focus on the nose and mouth. The best facial recognition system is to mimic human eye. In this scenario, weighting different facial components in a more proper way is very important. Note, we even saw these phenomena in our own laboratory, Table 4.1 shows example sketches when we asked members of our laboratory to sketch other members of the laboratory that were of a different race.

One of real world application of facial recognition is helping determine the identity of criminals. Sometimes, victims need to memorize and recall the face of criminals. In that case, it is not easy for people to remember every detail of the criminals' face; they will capture the most obvious facial feature. Considering memorizing limitation, a weighting model can be designed to address these problems.

Table 4.1 Example of Sketches drawn by different races people

| Real Facial Image | Sketch drawn by Caucasian people | Sketch drawn by Asian people |
|---|---|---|
|  |  |  |

We envision this work being used to be used in applications that will search images for matches against missing children or helping to track down escaped or wanted criminals. This work can help law enforcement agencies find the missing child or criminal by comparing last known images of the person to databases of images captured through websites or social media sites. Even after many years may have passed, some facial components can be considered the same while other features may change dramatically.

### 4.2. Hybrid region weighted model

Based on our stated application goals, our system is designed to utilize a hybrid approach, instead of striving for a holistic description. Furthermore, the local feature based hybrid methods can be more robust against variations in the subject's pose.

There is no doubt that some facial features (such as eyes, nose and mouth) have more contribution for human facial recognition than other features. Thus, the original histogram, which is explained in chapter 3, derived from log-LBP can be extended into a weighted region

enhanced histogram. This model focuses on both the appearance and the spatial relations of facial regions. See Figure 4.1 for two examples of a facial image divided into 3×3 and 4×4 rectangular regions.

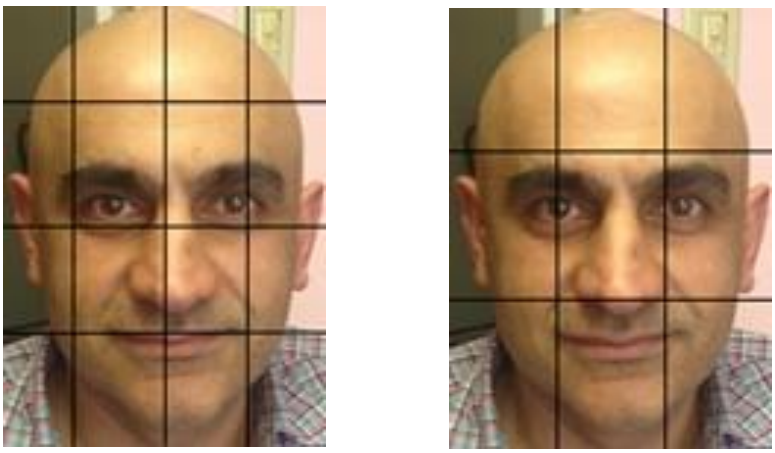

Figure 4.1 A facial image divided into 4×4 and 3×3 rectangular regions.

It should be noted that when using the histogram-based methods, the description of the face is no longer based on a pixel-level. Instead, this kind of description focuses on producing information on a regional-level. Then all regional patterns are concatenated to build a global description of the face.

The regions can be weighted based on the importance of the information they contain. Therefore, the enhanced histogram can be calculated by weighted Chi square statistic[86], which can be defined as:

$$\chi^2_\omega(x,\xi) = \sum_{j,i} \omega_j \frac{(x_{i,j} - \xi_{i,j})^2}{x_{i,j} + \xi_{i,j}} \tag{4.1}$$

In which x and $\xi$ are the normalized enhanced histograms to be compared, i and j refer to i-th bin in histogram corresponding to the j-th local region and $\omega_j$ is the weight for region j.

The proposed block diagram of a recognition system that tries to mimic the region-based recognition behavior is shown in Figure. 4.2. After decomposing the input image into its 16 different regions, the component features are extracted and weighted before being sent into the "decision making" process.

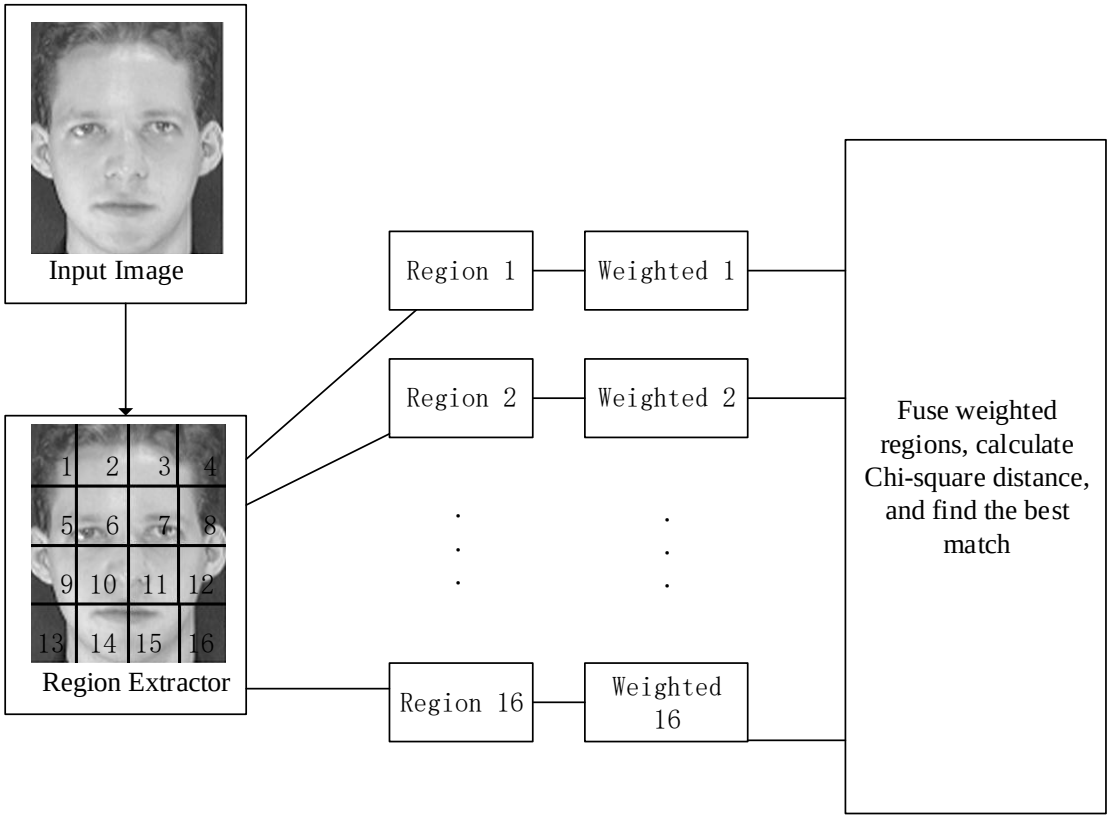


Figure 4.2 Block diagram of the hybrid weighted model

### a. Experimental simulation

In this section, we assess the performance and resolve the weighted parameters values by using images from the AT&T database, Yale database, ORL database and FERET database.

All these databases are commonly used public databases [87]. The FERET program set out to establish a large database of facial images that was gathered independently from the algorithm developers.

The Yale database Contains 165 grayscale images in GIF format of 15 individuals. There are 11 images per subject, one per different facial expression or configuration: center-light, with glasses, happy, left-light, wearing no glasses, normal, right-light, sad, sleepy, surprised, and winking an eye.

The AT&T database contains ten different images for each of 40 distinct subjects. For some subjects, the images were taken at different times, varying the lighting, facial expressions (open or closed eyes, smiling or not smiling) and facial details (with glasses or without glasses). All the images were taken against a dark homogeneous background with the subjects in an upright, frontal position (with tolerance for some side movement).

The ORL dataset that contains 400 images corresponding to 40 subjects. The ORL face database was developed at the Olivetti Research Laboratory, Cambridge, U.K. The variations of the images include different poses, sizes, time, and facial expressions.

Based on the public databases, each facial image is standardized to be a size of 112×92. The image is divided into 16 equal blocks of size 28×23. Then, all the LBP features are weighted based on the importance of the information they contain. LBP features are extracted from each of these blocks and concatenated to form the final feature vector for the facial image. For a uint8 image, 58 of the 256 possible 8 bit patterns are uniform and the non-uniform patterns are all put in the 59th bin. Hence the total length of the feature vector is 59×16 = 944. In this thesis, the Chi-square distance statistic has been used for calculating the similarity of facial images in our experiments.

The first step is to find the contribution for the facial recognition rate for each region. By setting other regions to "no contribution", we can get the single contribution of every region by seeing how many correct recognition decisions are made using just that single region. The result shown in table 4.2 is obtained by testing images of AT&T database.

Table 4.2 Single region contribution to determine how many correct recognitions are made using only the selected single region, while all others are set to no contribution

| Region Number | 1 | 2 | 3 | 4 | 5 | 6 | 7 | 8 |
|---|---|---|---|---|---|---|---|---|
| Recognition Rate (%) | 5 | 45 | 38 | 3 | 56.5 | 62.5 | 64 | 51.5 |
| Region Number | 9 | 10 | 11 | 12 | 13 | 14 | 15 | 16 |
| Recognition Rate | 50 | 43.5 | 40.5 | 41.5 | 2 | 36.5 | 40 | 0 |

We can easily see that there are four regions that have almost no contribution to the entire system recognition rate. And there are several regions that have similar contributions to the system recognition rate.

Hence, we adjust the original regions into 7 different new regions based on their single recognition rate. The figure 4.3 shows the new regions for the weighted method. The same color means the regions have the same weight.

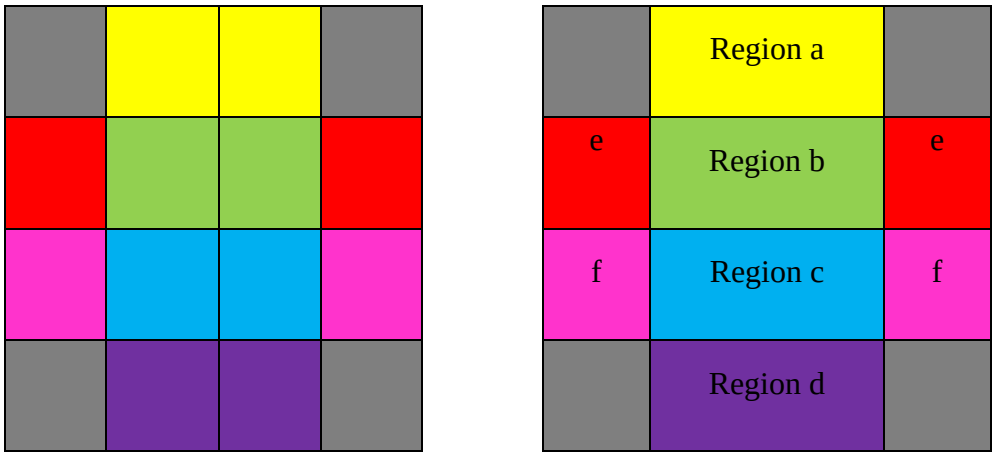


Figure 4.3 Modified weighted region, where the same colors indicate regions with the same weights

Based on the separated regions, we will find the contribution for the facial recognition rate for each region. By setting other regions to no contribution, we can get the single contribution of every region. The result shown in table 4.3 is obtained by testing images of AT&T database.

Table 4.3 Modified region contribution

| Region | a | b | c | d | e | f | gray |
|---|---|---|---|---|---|---|---|
| Recognition rate(%) | 46.5 | 64.5 | 52 | 46.3 | 68.5 | 60 | 0 |

**b. Experimental Results**

In this section, we will present the method to adjust weighted parameters based on the considering the single contribution and the modified region contribution. Below is a table of the most typical parameters selection and the corresponding recognition rate. The weighted values are multiplied by the log-LBP results of the modified region in table 4.4.

Table 4.4 Group of weighted value for experimental results

| Region Name | a | b | c | d | e | f | gray |
|---|---|---|---|---|---|---|---|
| Recognition Rate(Single) | 46.5 | 64.5 | 52 | 46.3 | 68.5 | 60 | 0 |
| Weighted Value 1 | 1 | 1 | 1 | 1 | 1 | 1 | 0 |
| Weighted Value 2 | 1 | 1.25 | 1.25 | 1 | 1.25 | 1.25 | 0 |
| Weighted Value 3 | 1 | 1.5 | 1.25 | 1 | 1.5 | 1.5 | 0 |
| Weighted Value 4 | 1 | 3 | 1.25 | 1 | 3 | 1.5 | 0 |
| Weighted Value 5 | 1 | 4 | 1.5 | 1 | 4 | 2 | 0 |

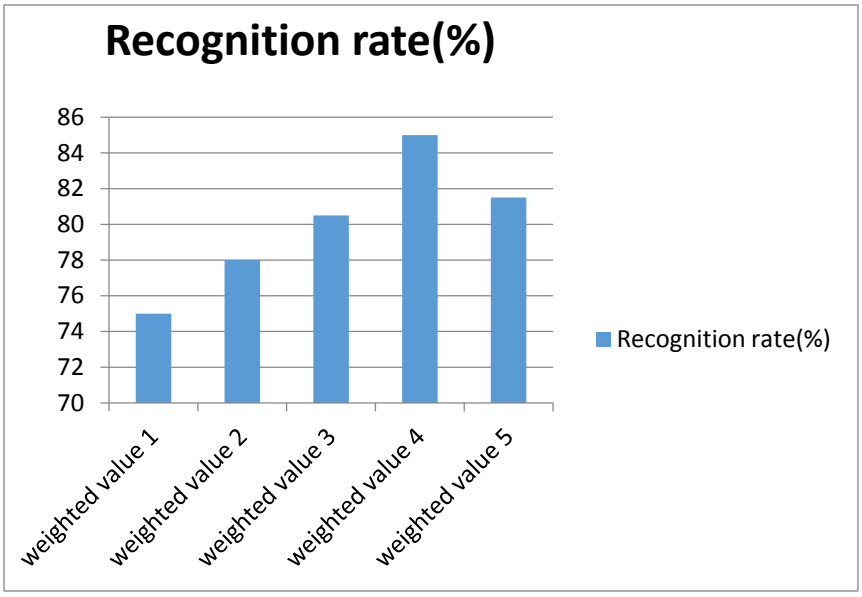


Figure 4.4 Recognition rate comparison based on table 4.3

The Weighted values in table are derived by considering the single contribution of each region. So according to the single regional recognition rate, we can easily find that region b and c play more important roles than region e, f and d. The region a is the least important. It makes sense that the most important features (such as eyes, nose and mouth) are located in region b and c. The recognition result of the different sets of weighted is shown in Fig4.4. The results were tested using different sets of values in Table 4.4.

To produce the highest result based on the hybrid region approach, we adjusted all the weighted values for the six different regions for 15,000 different sets of value. Then, we tested all sets of weighed values on different public databases. We put ten different images of a same person in varying poses, facial expressions and lighting conditions in the training group, and one different

image of that person in the testing group. The goal is to find all ten different images of the same person.

The recognition example result is shown below:

Table 4.5 Recognition results comparison of the non-weighted and hybrid method

| Non-weighted | | Weighted(hybrid) | |
|---|---|---|---|
| Testing image | Identified image | Testing image | Identified image |
|  |  |  |  |
|  |  |  |  |
|  |  |  |  |

After exhaustively testing different weighted values, we achieve a highest recognition rate of 85%. We have improved the original recognition rate from 75% to 85%.

We know that in the table.4.4 above, the first set of weighted value (1:1:1:1:1:1) is actually the original non-weighted classification. Hence, it can be observed that our hybrid region weighted model improved the non-weighted method by 15%.

### 4.3. Hybrid-Holistic region weighted model

Another proposed region weighted model is combining the hybrid method with the holistic method. The proposed model is shown in the diagram is shown in Figure 4.5.

First, we can extract the whole facial image features using LBP and generate a single vector for recognition.. Next, each facial region's feature vector is derived. Next, we use the Chi-Square statistic to locate the most similar training images. In addition, we score the most similar training image for each region based image feature for its own contribution and the most similar training image for the whole image to form the output.

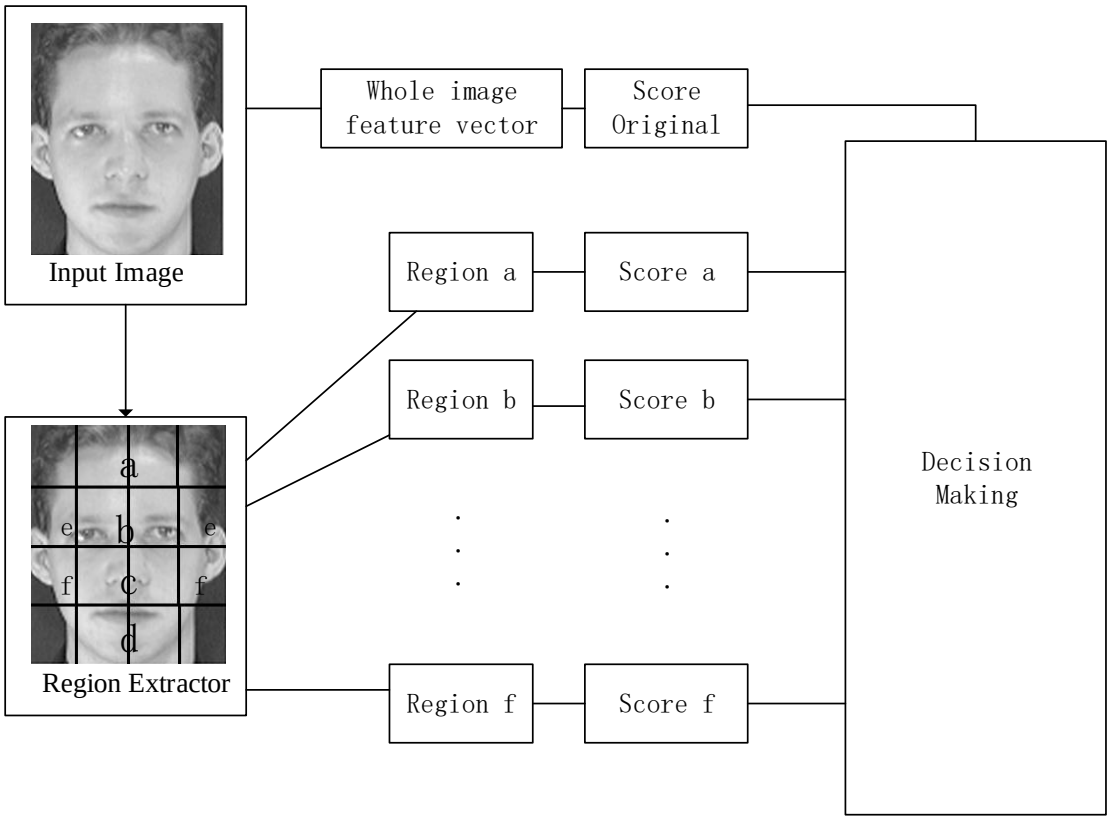


Figure 4.5 Block diagram of the combined weighted model

In the final decision making stage, we compare the fused scores of those selected "most similar" images and choose the best matching image which gets the highest score.

By combining the complete feature information with the regional feature information we can provide the advantage of robustness that can compensate for varying pose and illumination. This works on the premise that some of the facial regions may not be degraded drastically by the changes in pose, illumination or age conditions.

### a. Experimental simulation

Fig. 4.6 shows the recognition performance of the whole image feature and Regional features methods for the selected images of this experiment. Among the facial features, region b, c, d and e component had the maximum discrimination power. The facial regions can be sorted by decreasing performance as follows: Region b; Region e; Region f; Region c; Region d; Region a.

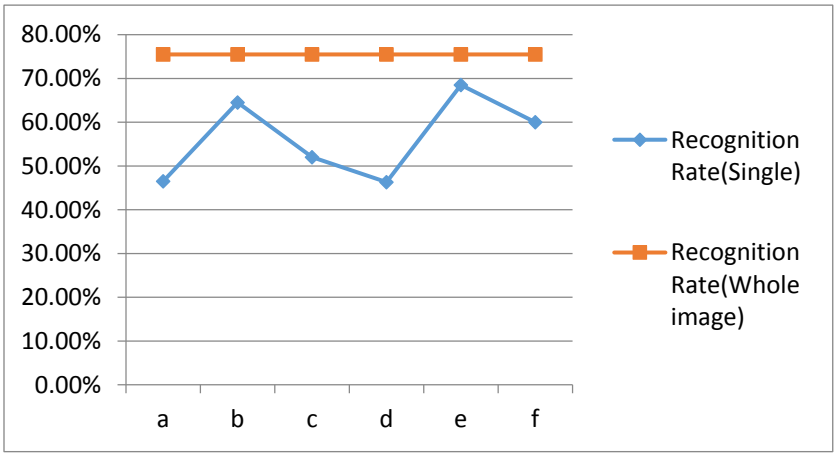


Figure 4.6 Recognition performance of the whole image feature and regional features

Based on the single regional recognition rate and the holistic facial recognition rate, we adjust the weighted score for each component. The weighted values for the scores of both the regions and the whole image are shown in table 4.6.

Table 4.6 Group of score value for experimental results

| Name | Whole image | Region a | Region b | Region c | Region d | Region e | Region f | Recognition Rate |
|---|---|---|---|---|---|---|---|---|
| Score Value | 5 | 0 | 0 | 0 | 0 | 0 | 0 | 75% |
| | 2 | 2 | 2 | 2 | 2 | 2 | 2 | 82.5% |
| | 5 | 1 | 3 | 3 | 1 | 2 | 2 | 88% |
| | 5 | 1 | 3 | 3 | 3 | 2 | 2 | 87.5% |
| | 5 | 1 | 4 | 4 | 1 | 1 | 1 | 87% |

To produce the highest result based on hybrid-holistic region weighted model, we adjust the score values for the six different regions and for the holistic image. We then tested all sets of weighed values on different public database. We put ten different images of a same person of variant poses, facial expression and lighting condition in the training group, and one different image of that person in the testing group. The goal is to find all ten different images of the same person.

After testing, we achieved the highest recognition rate, 88%. Compared with non-weighted approach, our Hybrid-Holistic Region Weighted Model improved the recognition rate from 75% to 88% experimentally.

### b. Experimental Results

Here, we show some example results using hybrid-holistic region weighted method.

Table 4.7 Recognition results comparison of non-weighted and our hybrid-holistic method

| Non-weighted | | Weighted(hybrid-holistic) | |
|---|---|---|---|
| Testing image | Identified image | Testing image | Identified image |
|  | 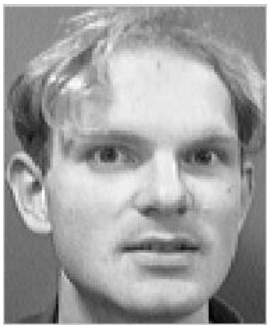 |  | 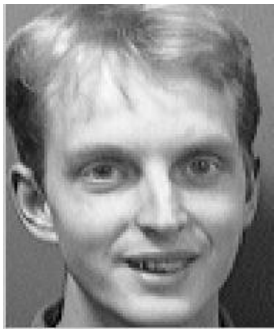 |
|  | 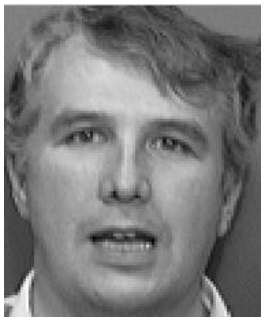 |  |  |
|  |  |  |  |

### 4.4. Comparison for weighted models and non-weighted method

The facial recognition rate results comparison is shown in Table 4.8 and Fig 4.7:

Table 4.8 facial recognition rate results comparison

| Region Name | Non-weighted | Hybrid weighted model | Hybrid-Holistic weighted model |
|---|---|---|---|
| Recognition Rate | 75.00% | 85.00% | 88% |

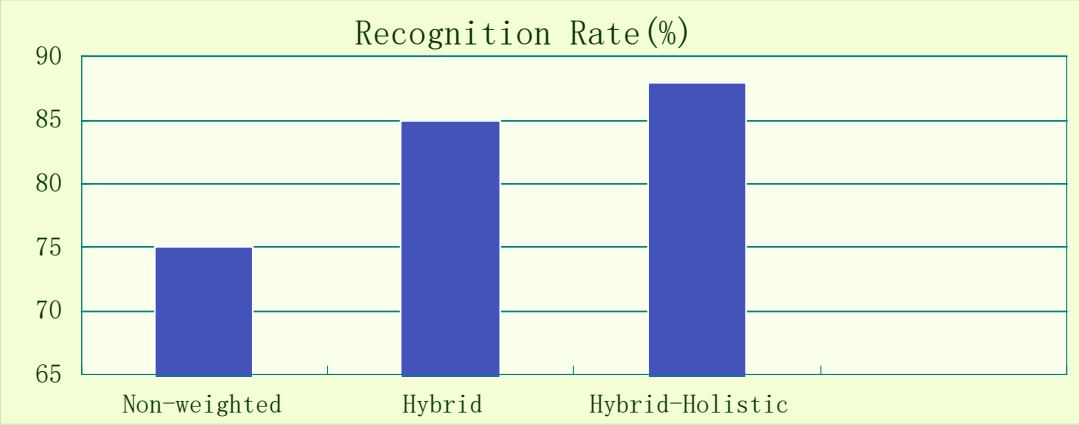


Figure 4.7 Non-weighted and Weighted method comparison

In this chapter we investigated non-weighted methods and formulated a weighted method that utilized both the region contributions as well as the overall image (holistic) recognition rate contribution.

# CHAPTER 5

## 5. FACIAL RECOGNITION BASED ON THE HUMAN VISUAL SYSTEM FOR ANTONOMOUS SYSTEMS

Facial recognition is considered to be a high priority topic in autonomous systems. In human visual systems, we aim to mimic the most basic processes of human nature, specifically facial recognition, which is one of the first things a child learns. Facial recognition is most widely applied in identification and authentication, since the human face can be easily captured by any imaging sensor such as a camera.

This section presents a real-time facial recognition system utilizing our human visual system algorithms. Our novel recognition approach computes a description of weighted facial regions based on the combination of the properties of the Human Visual System (HVS) and Local Binary Patterns (LBP). It aims to provide a similar performance as human eyes, the best existing facial recognition machine, in a low-cost, accurate and efficient manner**.** The architecture can quickly find and rank the closest matches of a test image to a database of stored images.

Our methodology produces a low cost and efficient detection and recognition of key features. For our prototype application, we supplied the system testing images and found their top- three matches in the database of training images. In addition, the results were further improved by

weighting the contribution of the most distinctive facial features. The system evaluates and selects the best matching images using a chi-squared statistic.

There are many potential applications for this work, including homeland security applications such as identifying persons of interest and other robot vision applications such as search and rescue missions.

### 5.1. Human Visual System based facial recognition

In this section, we present a short review of current facial recognition algorithms and describe our system architecture using LBP and HVS, as well as its advantages over other methods.

#### 5.1.1. Review of current facial recognition approach

Many facial recognition representation approaches have been developed. They are Principle Component Analysis (PCA), Linear Discriminate Analysis(LDA), Independent Component Analysis(ICA), and Gabor wavelet features. They all focus on reducing set of orthogonal basis vector or eigenfaces of training face images [88].

PCA[89] offers an optimal linear transformation from the original image space to an orthogonal eigenspace with reduced dimensionality in the sense of the least mean square reconstruction error.

ICA [47] is a generalization of PCA, which is sensitive to the high-order relationships among the image pixels.

LDA[90] seeks to find a linear transformation. It maximizes the between-class variance and minimizes the within-class variance.

Gabor wavelets features[91] capture the local structure corresponding to spatial frequency, spatial localization, and orientation selectivity.

In this thesis, we utilize a LBP facial recognition system algorithm to do the image representation. Timo et al proposed a novel approach for facial recognition, which takes advantage of the LBP histogram that is proven to be an effective texture description. In their method, experimental results show that the LBP outperformed other well-know approaches such as PCA, EBGM, and BIC on FERET database [52]. And also, it is shown that LBP is more robust against changing illumination and varying poses. Hence, we use the LBP description due to its robustness and efficiency.

After LBP processing, we use the Chi-square statistic to measure the similarity between testing images and training images, which is the difference between two histograms. While regarding other classification methods, like nearest neighbor[92], convolutional neural networks[93], nearest feature line[94], Bayesian classification[95] and AdaBoost[95] method, the Chi-square distance classification is more useful for simplifying computation and analysis.

### 5.1.2. Flow Diagram for Human Visual System based facial recognition

In this section, we will present our facial recognition system based on the analysis in 5.1.1, and describe the architecture.Generally, a typical automatic recognition system has three separate phases: training phase, testing phase and comparison phase. The flow diagram of a typical recognition framework is shown in Fig 5.1

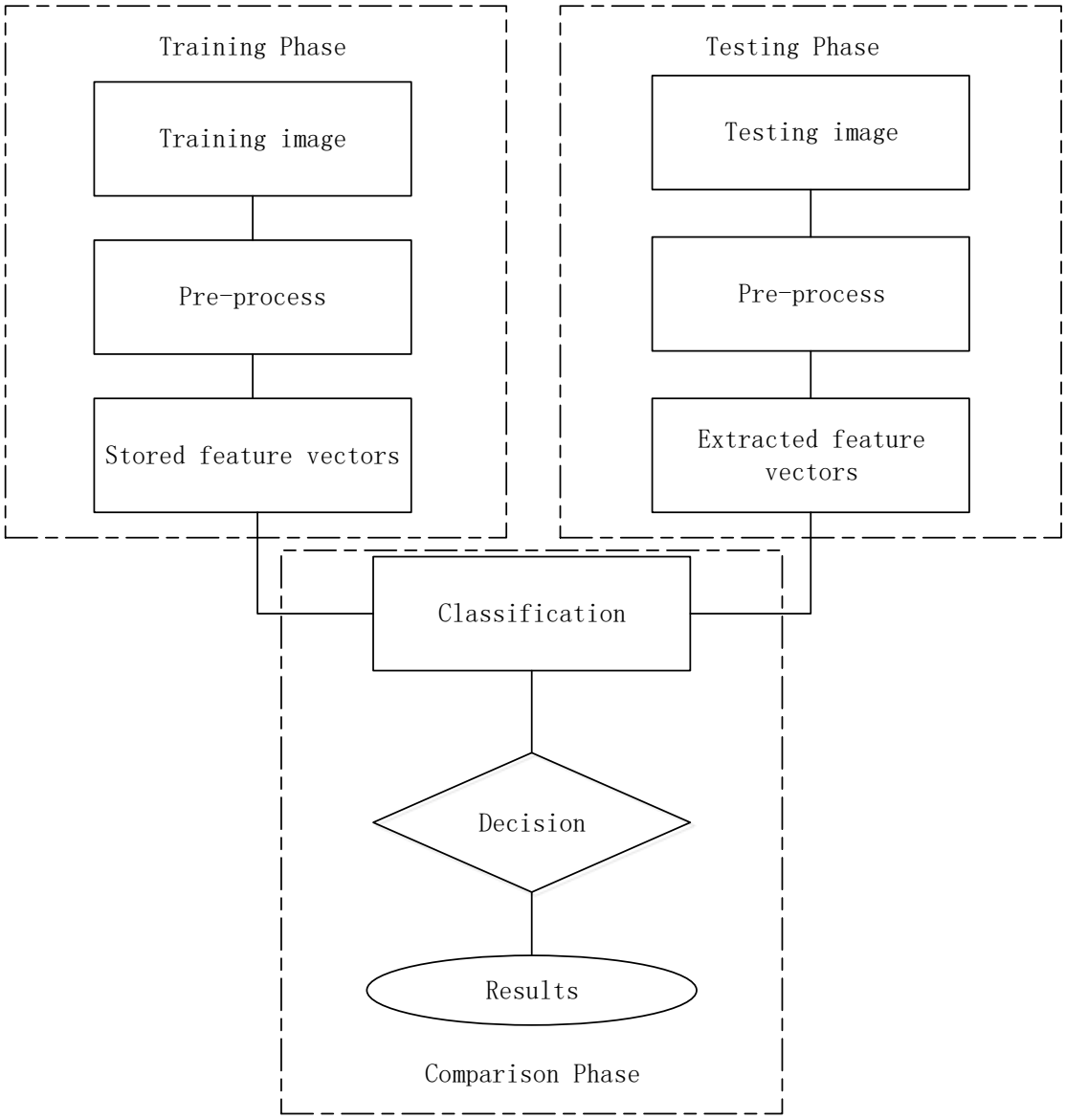


Figure 5.1 Flow diagram for a general recognition system

Our system architecture is accomplished based on the general schematic diagram for general recognition system, where the processing steps are implemented with our own novel algorithms. The flow chart of Human Visual System based facial recognition system is presented in Figure 5.2.

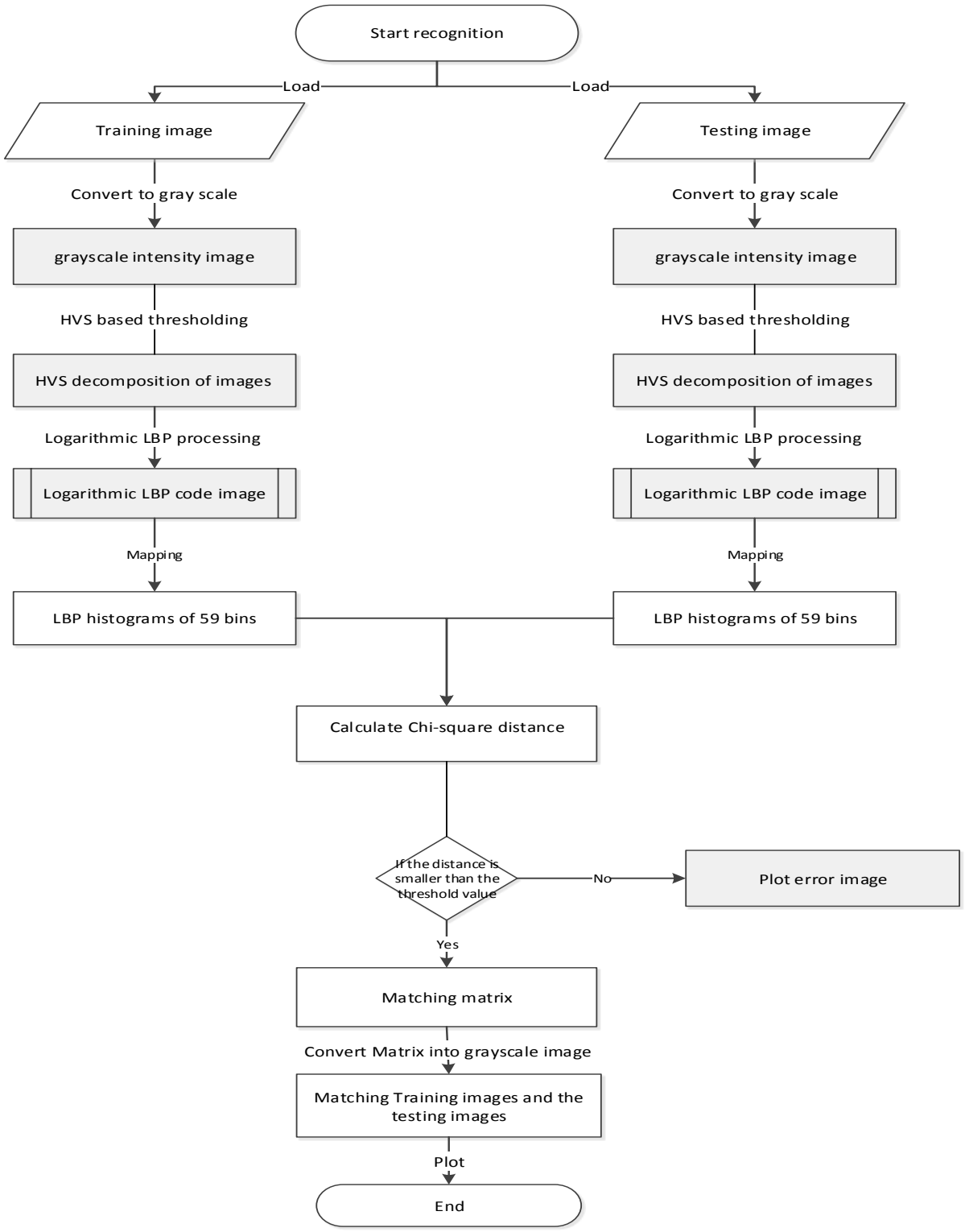


Figure 5.2 Flow chart for our Human Visual System based facial recognition system

Weighted HVS-LBP)

In the training phase, we use the Human Visual System model to decompose the training image. This results in decomposing the image into four different regions according to the Baushbaum curve, namely: Weber Region, De-Vries Rose Region, Saturation Region and Remaining Region. Next, we use a dynamic HVS thresholding method to get the ideal image. Additionally, we will utilize logarithmic Local Binary Patterns to generate the feature vectors of the training images. Feature vectors can be weighted according to the contribution of different facial components using two different weighted models, including the hybrid region weighted model and the hybrid-holistic region weighted model.

In the testing phase, we also apply the Human Visual System model to decompose the training image. We can get image in four different regions: Weber Region, De-Vries Rose Region, Saturation Region and Remaining Region. From our experiments we have found that majority information of an image is from the Webber Region, so we will combine information form Weber Region, De-Vries Rose Region and Saturation Region. Additionally, we will utilize logarithmic Local Binary Patterns to produce the feature vectors of the training images. Feature vectors will be weighted according to the contribution of different facial components.

In the comparison phase, we use the Chi-square statistic method to classify the feature vectors from training phase and testing phase. Then the similarity between two feature vectors will be calculated and the best or closest matches will be found.

## 5.2. Facial recognition Procedure

Our new novel architecture for HVS based facial recognition consists of four different procedures, which are the HVS based image decomposition, LBP-based facial recognition, classification and region weighting. Fig 5.3 is a refined representation of the entire system schematic diagram. We will explain each processing step in detail in this section of the thesis.

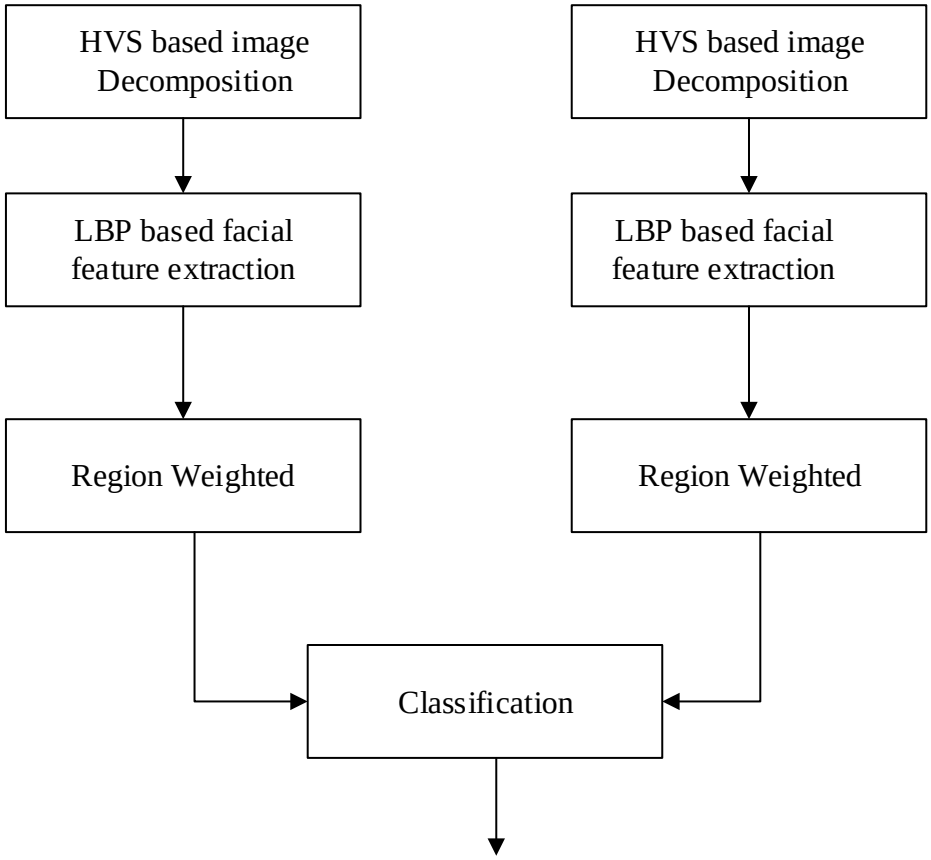


Figure 5.3 A refined representation of the entire system schematic diagram

### a. HVS Based Image Decomposition

HVS based image decomposition, which can segment the objects from their surroundings, provides a more accurate image pre-processing result.

In this stage, we first convert the input images into grayscale images. Then, we calculate the gradient magnitude and background information at each pixel in the grayscale images. Finally, by referring to HVS based thresholding rules explained in chapter 2, we can decompose the images into fore deferent sub-images, which are the Weber Region, the De Vries-Rose Region, the Saturation Region and remaining image pixels.

The thresholded images are given by representing the regions where human eyes can perceive a noticeable difference in intensity with respect to the image background. The last region “remaining image pixels” represents the regions in the image where the intensity values remain constant according to the human visual perception. In our experiment, it is efficient to fuse the Weber Region image ,De Vries-Rose Region image and Saturation Region image together for feature extracting since we could keep the more important information and facial localization features.

Here we will present two different types of fusion method.

**1) Arithmetic addition**

In this fusion case, we will simply add three thresholded images together. By doing this we can produce a corresponding result where human eyes can immediately perceive a noticeable change. Hence, our fusion process can be summarized as:

HVS decomposed image = Weber Region image + De Vries-Rose Region image + Saturation Region image (5.1)

**2) Parameterized Logarithmic Image Processing (PLIP) addition operators for image fusion[96]**

A second fusion method utilizes the Parameterized Logarithmic Image Processing operators for data fusion based on the Logarithmic Image Processing operators. The human eye processes logarithmically, so it is appropriate that we use logarithmic operations to emulate the human eye processing versus linear arithmetic. Researchers have introduced a set of operators that are based on this premise, including our own research group [97].

Sos Agaian, Karen Panetta, and Shahan Nercessian have introduced PLIP operators. PLIP addition is defined as[96] :

$$a \oplus b = a + b - ab/M \quad (5.2)$$

Here, M is the maximum value of the range.

In this fusion case, we will logarithmically add three thresholded images together. By doing this, we can generate a corresponding result where human eyes can perceive a noticeable change more accurately. Hence, our fusion procedure will be represented as:

HVS decomposed image = Weber Region image $\oplus$ De Vries-Rose Region image $\oplus$ Saturation Region image (5.3)

In this section, we will present two examples of the Human Visual System based image decomposition. We show the results using arithmetic addition, and applying logarithmic addition for the fusion process.

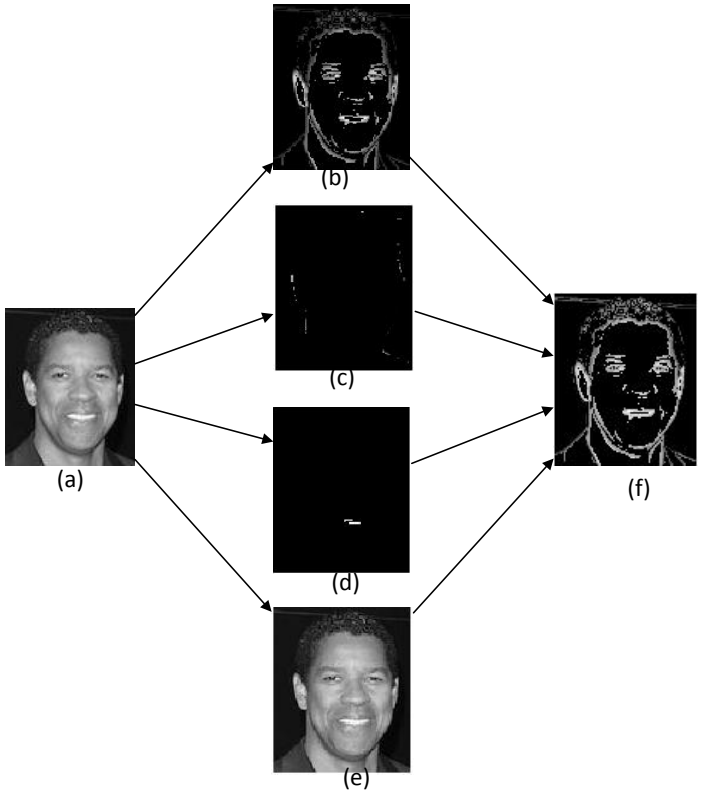


Figure 5.4 (a) Original Grayscale Image (b) Weber Region (c) De Vries-Rose Region (d) Saturation region (e) Remaining image pixels (f) Result of HVS-based thresholding Algorithm by Arithmetic addition

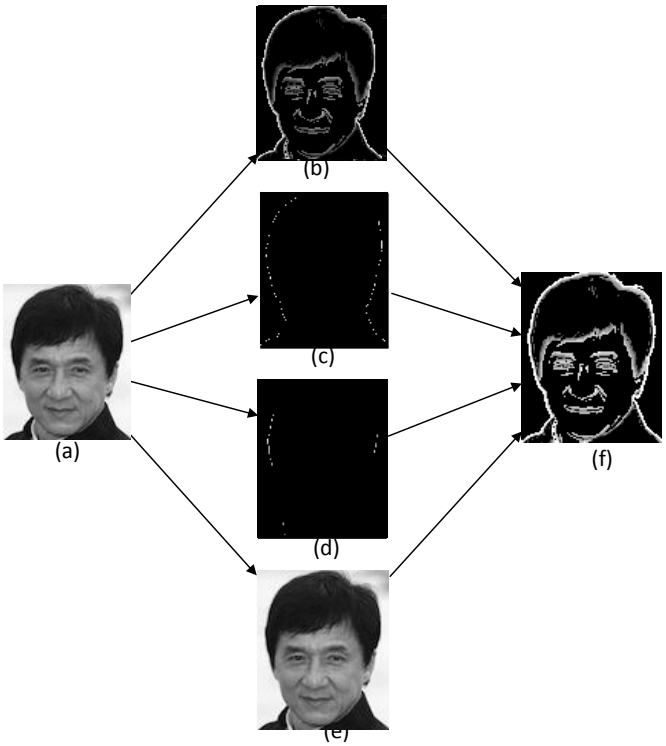


Figure 5.5(a) Original Grayscale Image (b) Weber Region (c) De Vries-Rose Region (d) Saturation region (e) Remaining image pixels (f) Result of HVS-based thresholding Algorithm by PLIP addition

**b. LBP-based facial recognition**

The Local Binary Pattern operator is robust to monotonic gray-scale changes, and its computational simplicity is also outstanding, which makes it possible to analyze images in challenging real-time settings. In our novel method, we transform the extracted LBP features from the logarithm domain. Figure.5. 6. depicts the flow chart of LBP processing**.**

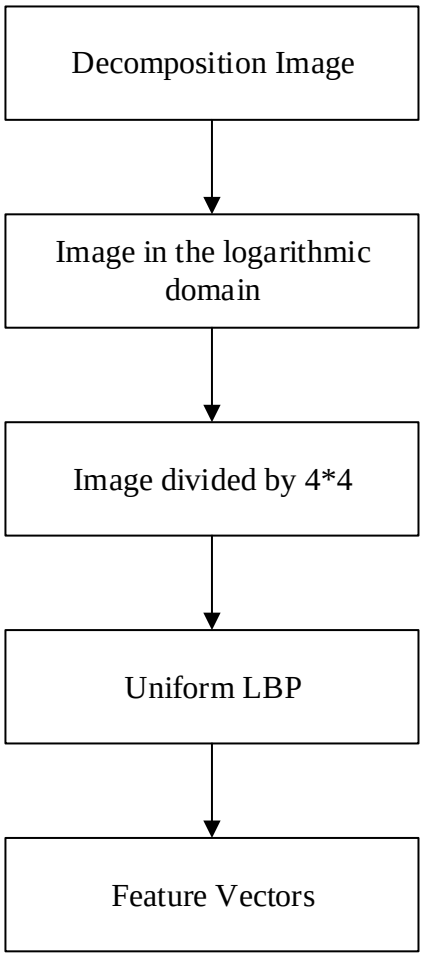


Figure 5.6 The flow chart of logarithm LBP features extracting process.

**c. Classification**

Classification is the process of categorizing a new observation to a set of known categories, on the basis of a training set of data. In a more general terms, classification is a decision based on comparing the similarity of the feature vectors of training and testing data. In our case, feature vectors are extracted from the training facial images that are already stored in the database and

compared to the testing images that are the input into the system. Then, the testing facial image is identified by comparing those feature vectors to the training feature vectors already stored.

Usually, in facial recognition, there are a number of face classes (representing an individual person) and a few training images per class. Hence, instead of using a sophisticated classifier, a nearest-neighbor classification approach is used. The different types of dissimilarity measures that can be used are detailed in [98] and summarized in Table 5.1:

Table 5.1 Dissimilarity Measures

| Histogram Intersection | Log-likelihood Statistic | Chi square statistic |
|---|---|---|
| $D(S,M)=\sum_i \min(S_i,M_i)$ | $L(S,M)=-\sum_i S_i \log M_i$ | $\chi^2(S,M)=\sum_i \frac{(S_i-M_i)^2}{S_i+M_i}$ |

For this stage, we determine the similarity by computing the Chi-square distance. Here $S_i$ and $M_i$ are the normalized histograms to be compared. For most of our experiments, the chi square distance statistic has been used since it is an effective measure of similarity between a pair of histograms.

The smaller the Chi-square distance value, the more similar the testing image is to the training image. Fig. 5.7 shows how we find the matching images from a large amount of training images in a database.

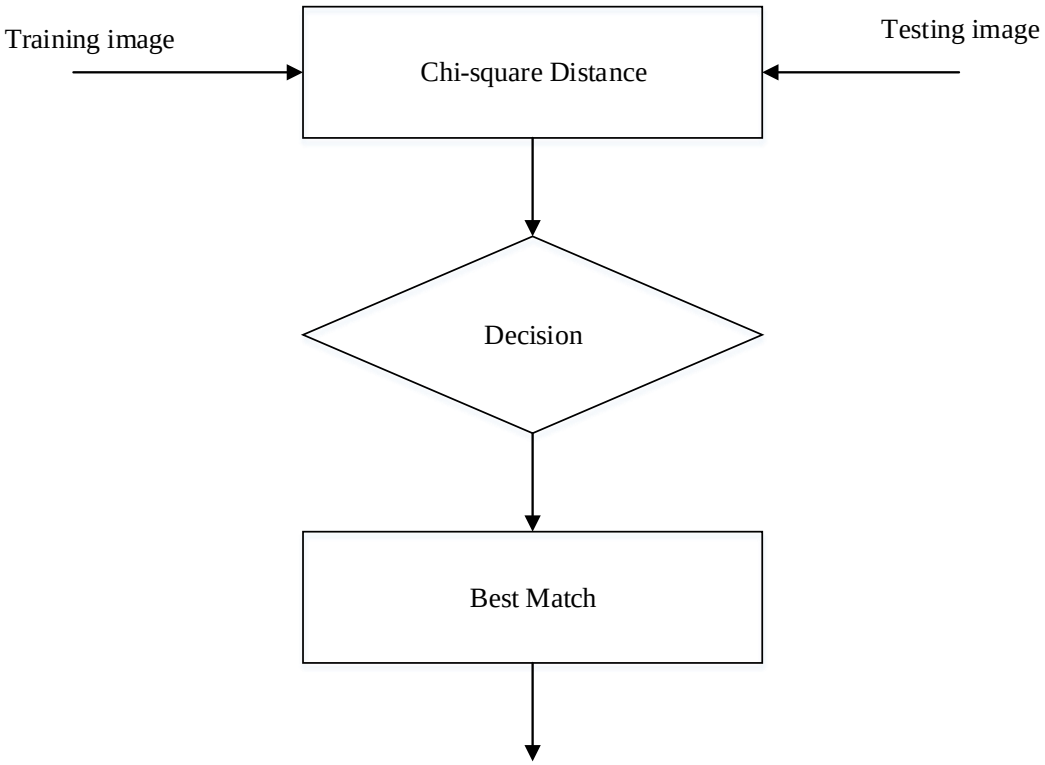


Figure 5.7 Diagram of Classification

**D. Region Weighted**

In this part, the log- $\mathbf{LBP}_{8,2}^{U2}$ operator in a 28×23 pixel window is selected since it is a good trade-off between recognition performance and feature vector length. When comparing different distance measures, the $\chi^2$ (chi-square statistic)measure was found to perform better than histogram intersection or log-likelihood distance. Therefore, the $\chi^2$ measure was chosen to be used.

To find the weights $\omega_j$ for the weighted $\omega_j$ statistic, a simple procedure was applied in which a training set was classified using only one of the 28×23 windows at a time and the

windows were assigned a weight based on the recognition rate. Fig. 5.8 shows the weights settings for our facial recognition system.

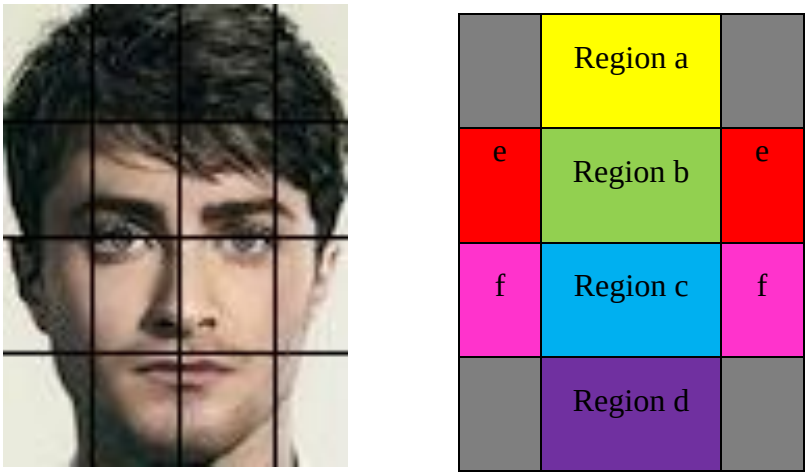


Figure 5.8 Example of weights setting

In Fig 5.9, (a) is an example facial image divided into 4×4 windows. And, (b) is the region set for the weighted dissimilarity measure. We apply two weighted models that are explained in chapter 4: i) Hybrid weighted model, the weighted value for region a, region b, region c, region d, region e and region f are 1, 3, 1.25, 1, 3, 5 respectfully; ii) Hybrid-Holistic weighted model, the weighted score for region a, region b, region c, region d, region e and region f are 1, 3, 3, 1, 2, 2 respectfully and the weighted score for the whole image is 5. These two sets of weighted parameters, which were obtained experimentally, achieved a high recognition rate.

## 5.3. Experimental Results

### 5.3.1. Experimental results for the Weighted HVS-LBP Recognition System using public database

First, we will present the recognition rates for HVS based non-weighted model facial recognition system, HVS based Hybrid region weighted model facial recognition system and the HVS based Hybrid-Holistic region weighted model facial recognition system for the AT&T database, the Yale database and the FERET database.

Here we list a table of all the attributes of the public databases:

Table5.2Attributes for different public database

| Attributes / Database | Color | Pose | Expression | Brightness |
|---|---|---|---|---|
| AT&T database | Gray | No | Yes | Same |
| Yale database | Gray | No | Yes | Different |
| FERET database | RBG | Different body position | Yes | Different |

Table 5.3 the recognition comparison for HVS based facial recognition system (Non-weighted), HVS based facial recognition system (Hybrid-weighted) and HVS based facial recognition system (Hybrid-Holistic ) for three public databases

| Name / Public Database | HVS based facial recognition system (Non-weighted ) | HVS based facial recognition system (Hybrid-weighted ) | HVS based facial recognition system (Hybrid-Holistic ) |
|---|---|---|---|
| AT&T database | 75% | 85% | 88% |
| Yale database | 76% | 87.5% | 88.5% |
| FERET database | 70% | 82% | 85% |

Then, we will present some analysis of these facial recognition results using the AT&T, the Yale face database and FERET database. For different databases with different image sizes, we divide the images is into 16 equal blocks of same size. Then, we weighted all the LBP features based on the importance of the information they contain. LBP features are extracted from each of these blocks and concatenated to form the final feature vector for the facial image. For a uint8 image 58 of the 256 possible 8 bit patterns are uniform and the non-uniform patterns are all put in the 59th bin. Hence the total length of the feature vector is $59 \times 16 = 944$. Chi-square distance statistic has been used for majority of our experiments. Table.5.3, table 5.4 and table 5.5 show the recognition results for the missed recognitions using Non-weighted and how using the Hybrid

region weighted model and Hybrid-holistic region weighted model, true recognitions can be obtained.

Table 5.4 the recognition results of AT&T database

| **Testing Image** | **Identified image** | | |
|---|---|---|---|
| | HVS based facial recognition system (Non-weighted ) | HVS based facial recognition system (Hybrid-weighted ) | HVS based facial recognition system (Hybrid-Holistic ) |
|  |  |  |  |
|  | 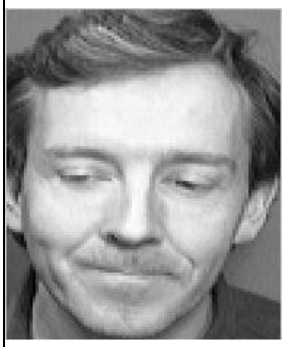 |  |  |
| 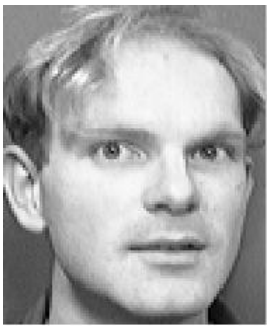 | 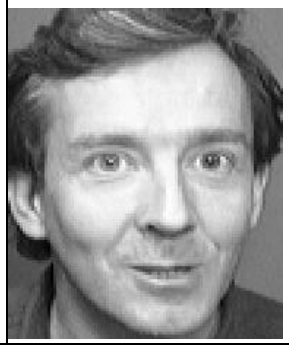 | 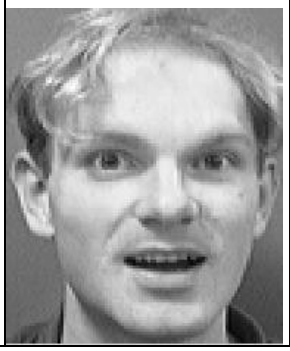 | 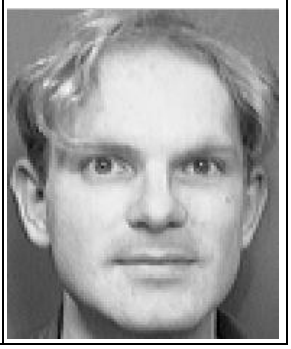 |

Table 5.5 the recognition results of Yale database

| **Testing Image** | **Identified image** | | |
|---|---|---|---|
| | HVS based facial recognition system (Non-weighted ) | HVS based facial recognition system (Hybrid-weighted ) | HVS based facial recognition system (Hybrid-Holistic ) |
|  |  |  |  |
|  |  |  |  |
|  |  |  |  |

Table 5.6 the recognition results of FERET database

| **Testing Image** | **Identified image** | | |
|---|---|---|---|
| | HVS based facial recognition system (Non-weighted ) | HVS based facial recognition system (Hybrid-weighted ) | HVS based facial recognition system (Hybrid-Holistic ) |
|  | 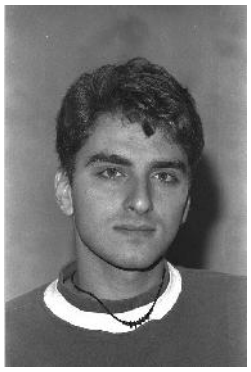 |  |  |
| 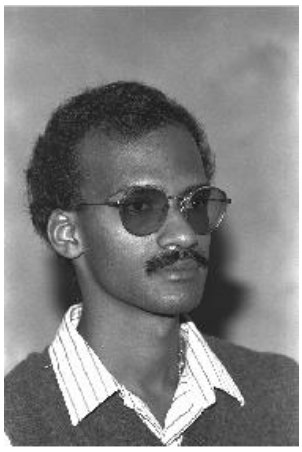 |  |  |  |
|  |  |  |  |

### 5.3.2. Experimental results for facial recognition application—What Celebrity do you most closely resemble?

To ensure the reliability of the tests, we used the IMDB[99] database as stored training images and 10 people from the general population as testing images. Those images contain variations in facial expression, and pose angles. The reason why we introduce this application of our Weighted HVS-LBP facial recognition system is that this system provide a way to address a lot of cases that we cannot accurately track the person of interest, for instance, finding missing children etc. The facial images can be divided into six sets as follows.

- Case 1: Frontal Face images (200 celebrities)
- Case 2: Face with facial expressions images(130 celebrities)
- Case 3: Male Face images (100 celebrities)
- Case 4: Female Face images (100 celebrities)
- Case 5: White and African Face images (168)
- Case 6: Asian Face images (32)

In all our experiments, logarithm-uniform LBP feature descriptors are used for feature extraction, which aims at creating faster computations. Each facial image in the database has a size of $112 \times 92$. The image is divided into 16 equal blocks of size $28 \times 23$. Then, we weighted all the LBP

features based on the importance of the information they contain. LBP features are extracted from each of these blocks and concatenated to form the final feature vector for the facial image. For a uint8 image 58 of the 256 possible 8 bit patterns are uniform and the non-uniform patterns are all put in the 59th bin. Hence the total length of the feature vector is 59×16 = 944. Chi-square distance statistic has been used for majority of our experiments.

Our experimental results were obtained by testing our facial recognition system with a varying number of testing and training images. The final results are shown in table 5.7 and table 5.8.

Table 5.7 Comparison of facial recognition rate of weighted models and non-weighted method

| Method | Frontal Face | Face with expression | Male | Female | Caucasian and Non-Caucasian | Asian |
|---|---|---|---|---|---|---|
| HVS Based LBP, hybrid-weighted | 92% | 80% | 86% | 82% | 83% | 79% |
| HVS Based LBP, hybrid-holistic weighted | 95% | 82.5% | 88% | 89% | 85% | 83% |
| HVS Based LBP, non-weighted | 75% | 66% | 71% | 71% | 69% | 62% |

The values in table 5.6 represents the percentage of agreement of human observers with the HVS system's assessment of image similarity. The results are displayed in figure 5.9.

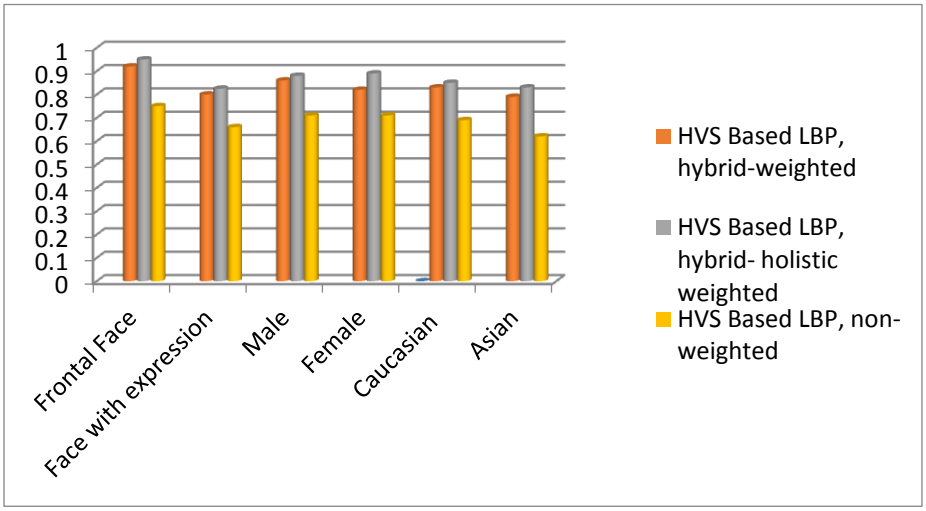


Figure 5.9 Comparison of the recognition similarity rates

Our experimental results were obtained by testing our facial recognition system with a varying number of testing and training images. The final results are shown in Fig. 5.10. and Fig 5.11. For every person, we output the five most likely people and the similarity rate is shown below.

Table 5.8 Example recognition of HVS Based LBP facial recognition system, hybrid-weighted model

| | | | | |
|---|---|---|---|---|
|  |  |  |  |  |
| Similarity | 99.97% | 87.378% | 85.075% | 82.012% |

| | | | | |
|---|---|---|---|---|
|  |  |  |  |  |
| Similarity | 99.085% | 94.9728% | 88.672% | 85.747% |
|  |  |  |  |  |
| Similarity | 100.000% | 98.637% | 94.672% | 87.885% |

Table 5.9 Example recognition of HVS Based LBP facial recognition system, hybrid-weighted model

| | | | | |
|---|---|---|---|---|
|  |  |  |  |  |
| Similarity | 99.97% | 89.672% | 89.039% | 84.127% |
| 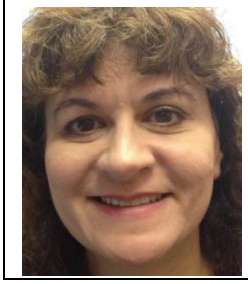 |  |  |  |  |

| | | | | |
|---|---|---|---|---|
| Similarity | 99.085% | 87.297% | 84.659% | 82.010% |
|  |  |  |  |  |
| Similarity | 100.000% | 98.637% | 94.672% | 87.885% |

# CHAPTER 6

# 6. APPLICATIONS FOR AUTOMATED FACIAL RECOGNITION BASED ON HUMAN VISUAL SYSTEM

Automated facial recognition has made huge progress recent years; hence more and more real-life applications based on facial recognition system are being developed. In this section, we will focus on exploring real-life applications using automated facial recognition system based on human visual system and region weighted models.

First, we will present an automatic recognition system for matching composite sketches to facial photos. To our knowledge, the research area has not been well studied. We will discuss this application in details.

Next, we will apply our facial recognition system to implement the recognition case for age tracing. We believe our prototype system will be of great value to law enforcement agencies to help combat human trafficking as well as finding missing children and wanted criminals.

Finally, we will also implement our HVS based region-weighted facial recognition system for animal recognition. This can be used to find lost pets, which is intended to show the applicability of the weighted method for other "faces" even if they are not human.

### 6.1. Automatic Recognition system for Matching Composite Sketches to Face Photo

Though automated facial recognition has made dramatic progress and it has been well studied for one of its important applications, namely to help determine the identity of criminals, challenges still occur when the facial photographs of the suspect are not available. In this case, drawing a sketch from a description provided by an eyewitness or the victim is a commonly used method to assist the police to identify possible suspects [7]. In fact, criminal investigations have leveraged face sketches as far back as the late 19th century [100] [101].

However, due to budgetary reasons, most law enforcement agencies use facial composite software instead of hiring a professional artist. These existing facial composite software programs allow the user to create a computer generated facial composite (composite sketch) [101].

Here, we will present some examples of sketches. Fig. 6.1 (a), (b), (c) show three cases reported in the media, where suspects were successfully identified through forensic sketches drawn by artists. Figure. 6.1 (d), (e), (f), shows three different cases in which suspects were identified based on computer generated composite sketches. Those are examples based on recent research [7]. In Figure 6.1 (a) is drawn based on descriptions provided by the female victims led to arrest of suspect in Virginia Highland armed robbery.[102] (b) A police sketch helped identify a man

suspected of attacking a woman on a street [103]. (c) Forensic sketch by face reconstruction led to identification of the victim in a possible murder [104]. (d) Composite sketch created using FACES aided in identifying the culprit of several armed robberies [105]. (e) Composite sketch created using SketchCop® led to the arrest of a suspect that attacked several female drivers[106]. (f) Composite sketches created using SketchCop led to arrest of an escaped suspect [107].

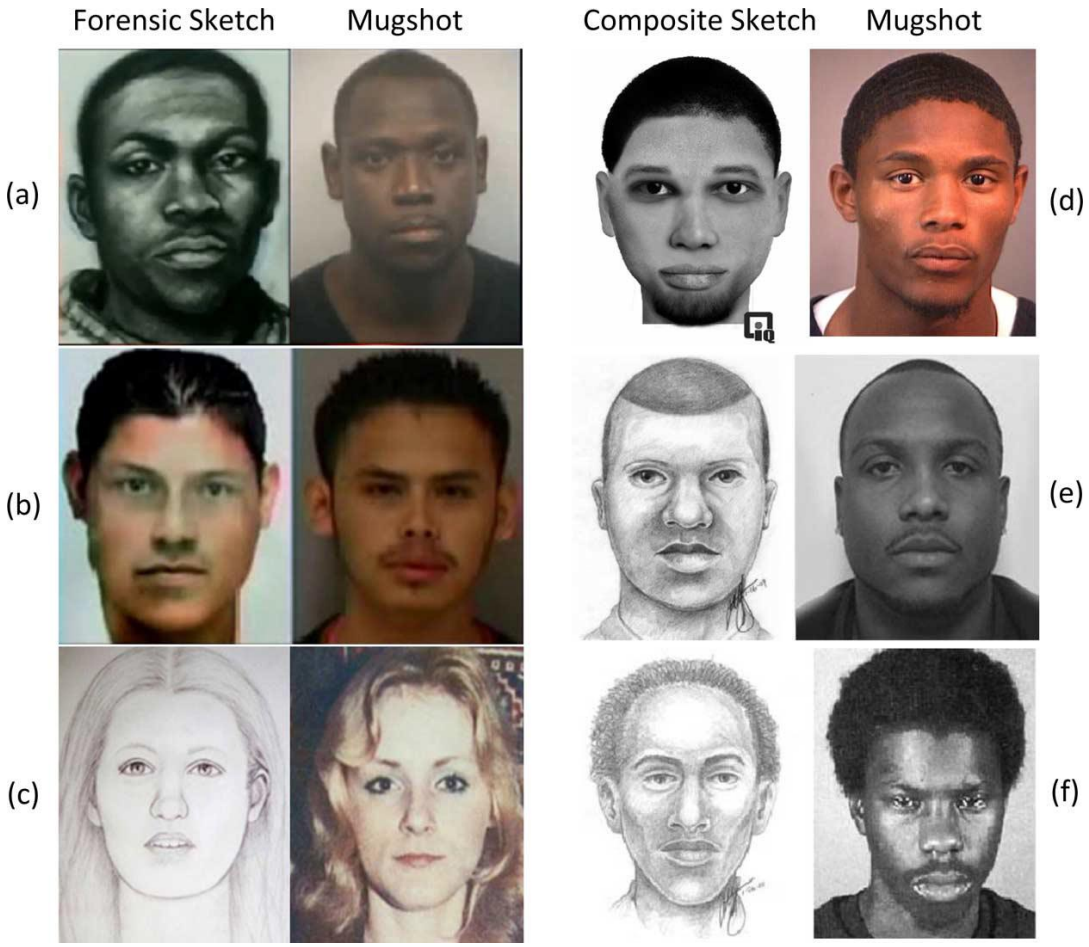


Figure 6.1 examples based on recent research for matching sketches to facial photos

Although several methods exists for matching hand drawn sketches to photographs appearing in the literature, to our knowledge, there has been only limited research on matching computer generated composites to mugshot photographs [108].

This section investigates the use of the HVS-based automatic recognition system to successfully match composite sketches to mugshots. This would aid in quickly and accurately identifying suspects involved in criminal activities.

### 6.1.1. Flow Diagram of Human Visual System based sketch-facial recognition

Fig 6.2 is the flow diagram of the recognition system for Matching Composite Sketches to Facial photo.

Including sketches in our facial recognition system can be separated in to five steps:

1) Load the facial images and sketches and then convert them into grayscale images;
2) Apply Human Visual System image decomposition and fusion of the sub-images to create a grayscale edge map;
3) Applying the Logarithm-Local Binary Pattern to obtain the LBP coded image;
4) Using Hybrid-Holistic Region Weighted model get the improved regional histogram;
5) Calculating Chi-square distance and matching the top-3 likely facial images according to the input sketches.

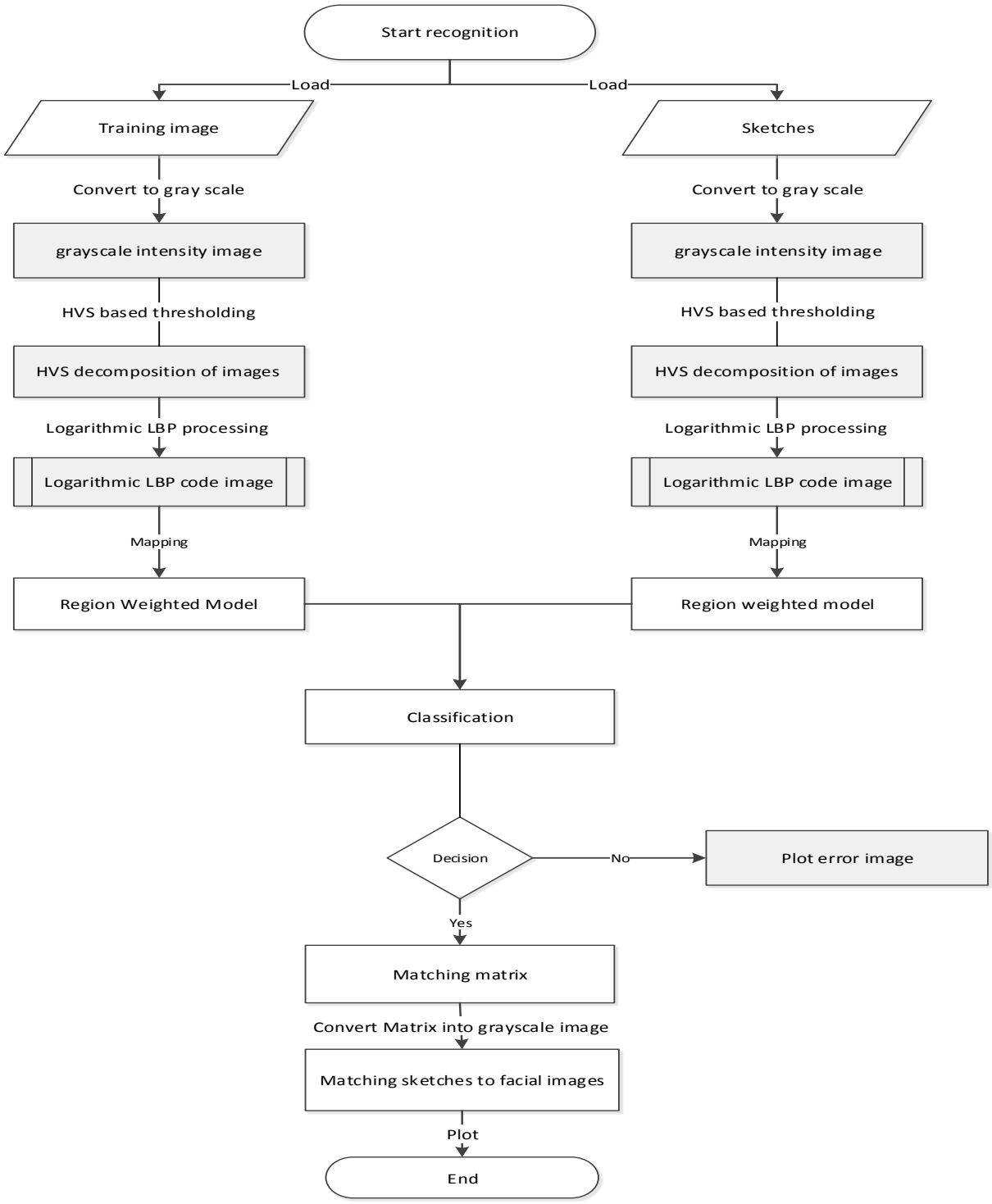


Figure 6.2 Flow chart for the HVS sketch-facial image recognition system

### 6.1.2. Sketch-Facial recognition system simulation procedure

In this section we will present the facial sketch making procedure and the sketch-facial image recognition simulation procedure. In Figure 6.3, we show the steps to take a picture of Dr. Karen Panetta, our laboratory Director and create a sketch from her photogram.

(a) 

(b) 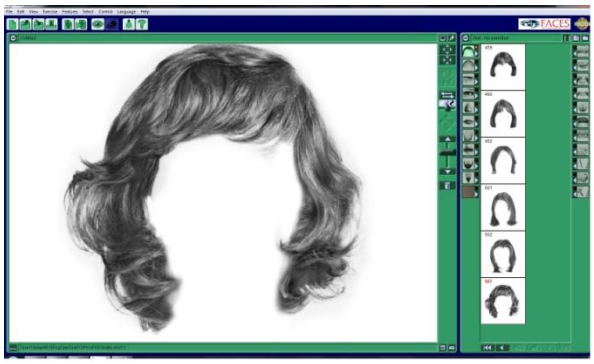

(c) 

(d) 

Figure 6.3 (a) is the original image, (b) (c)and (d) is the procedure for creating Dr.Karen Panetta's composite sketch using FACES [105]

### 6.1.3. Sketch-Facial image recognition results

In this section, we will present example results for our HVS Sketch to Facial image recognition system. First, we apply our sketch-facial image recognition system to a public database, CUHK Face Sketch database (CUFS) is for research on face sketch synthesis and face sketch recognition[107]. It includes 188 faces from the Chinese University of Hong Kong (CUHK) student database, 123 faces from the AR database, and 295 faces from the XM2VTS database. There are 606 faces in total. For each face, there is a sketch drawn by an artist based on a photo taken in a frontal pose, under normal lighting condition, and with a neutral expression. Table 6.1 shows the recognition results of sketch-facial recognition results.

Table 6.1 Example results of CUHK Face Sketch database

| Testing Sketch | Identified Image | Testing Sketch | Identified Image |
|---|---|---|---|
|  |  |  |  |
|  |  |  |  |
|  |  |  |  |

Then we will present the simulation results of our own database of Tufts University Panetta Imaging and Simulation Lab. This database is created based on the members of our Lab. Table 6.2 shows the original input sketch images and the top-three identified image.

Table 6.2 Example results of the Panetta Imaging and Simulation Lab Face Sketch database

| Testing Sketch | Identified Image(top 1) | Identified Image(top 2) | Identified Image(top 3) |
|---|---|---|---|
|  |  |  |  |
|  |  |  |  |
|  |  |  |  |
|  |  |  |  |

## 6.2. Missing Children application

Every year an estimated 800,000 children are reported missing[109]. Missing children has become a very serious problem and is exasperated by human trafficking; however there is no existing efficient and low-cost way to assist in these cases. We envision that using methods like this would allow parents to search the internet on their own using this more systematic method. In this section, we will apply our methodology to deal with the missing children problem.

We will make our prototype application based on celebrities' young images and older images from IMDB database. Table 6.3 shows some example results of matching the same person of childhood and older pictures. Since 10 years may change a lot of facial characteristics, we will show the top-three likely images produced by our system.

Table 6.3 Example results of Missing Children Problem

| Testing Image(kid) | Identified Image(top 1) | Identified Image(top 2) | Identified Image(top 3) |
|---|---|---|---|
|  |  Check |  Check |  Miss |

| | | | |
|---|---|---|---|
|  |  Miss |  Miss |  Check |
|  |  Miss |  Check |  Miss |

From the results, we can see that, after 10 years, many facial components have changed quite a bit for the same person. Our prototype method shows some validity to deal with missing children problem by applying our facial recognition system.

We also believe this shows promise for our automatic facial recognition system to be used to find wanted criminals. We believe our prototype facial recognition system has great value to law enforcement agencies in apprehending suspects in a timely fashion.

### 6.3. Pet finder application

In this section, we will utilize our facial recognition system to solve missing pets' problem. The goal of the application is intended to show our approach's applicability to finding other objects with faces to validate the weighted approach methodology. However, this case has many limitations. First of all, facial characteristics of an animal appear to possess much less uniqueness than a human, so this presents a challenge to find a suitable facial feature extraction algorithm. Next, for pets, their breeds, shape and fur offer other difficult challenges to the recognition problem. Here, we will present some example results of dogs form different breeds and cats from different breeds.

Table 6.4 Example results of Missing Dogs Problem of different breed

| Testing image | Training image | | | | | |
|---|---|---|---|---|---|---|
|  |  |  |  |  |  | |
| Result Identified image |  (check) | | | | | |

Table 6.5 Example results of Missing cats Problem

| Testing image | Training image | | | | | |
|---|---|---|---|---|---|---|
|  |  |  |  |  |  | |
| Result Identified image |  (check) | | | | | |

Table 6.6 Example results of Missing Dogs Problem of same breed

| Testing image | Training image | | | | | |
|---|---|---|---|---|---|---|
|  |  |  |  |  |  | |
| Result Identified image |  (miss) | | | | | |

Then, we will present some example results of dogs form same brand. The result is shown in table6.6. The result shows that it is not easy to find the target pets because of the similar shape and facial features.

From our exploration of a different usage of our facial recognition system, we can understand some of the limitations of our method, such as when trying to find animals the size, breed, fur color play an important role.

Despite this, we believe there is much promise for searching for non human faces and can envision future work in this area.

# CONCLUSION AND FUTURE WORK

A Weighted HVS-LBP facial recognition system has been introduced in this thesis. Because some facial regions are more effectual in facial recognition, we introduced two different region weighted models. It has been shown that it provides a better rate of detection and recognition compared to the non-weighted LBP-HVS based systems. Its efficiency, low-cost and robustness make this method suitable for many real-life applications. One of the applications is automatically matching composite sketches to facial photographs. Furthermore, other applications that could utilize this work include finding missing children or victims of human trafficking. Finally, we investigate the limitations of the system by applying the algorithms for other non-human facial features, namely matching animals.

In the future, we will improve our prototype facial recognition system by adding a facial detection module. Also, we will improve our limitation on fixed region weighted model into a automatic locating facial components weighted model. Moreover, we will focus on facial expression and information compensation using the Weighted-HVS-LBP based facial recognition system, and also develops an HCI, AI and apply the algorithm for more biometric technology applications.

## REFERENCES


[1]. A.Devi, *Image Processing Techniques in Face Recognition.* International Journal of Computer Trends and Technology, 2013. **4**: p. 59-62.

[2]. Zhao, W., et al., *Face recognition: A literature survey.* ACM Computing Surveys (CSUR), 2003. **35**(4): p. 399-458.

[3]. Davis, R. and R. Davis, *Magic Paper: Sketch-Understanding Research.* Computer, 2007. **40**(9): p. 34-41.

[4]. Chellappa, R., C.L. Wilson, and S. Sirohey, *Human and machine recognition of faces: a survey.* Proceedings of the IEEE, 1995. **83**(5): p. 705-741.

[5]. Dees, T. *Facial Recognition*. 2004. **52**, 26.

[6]. Grgic, M., et al., *EDITORIAL*. International Journal of Pattern Recognition & Artificial Intelligence, 2009. **23**(3): p. 355-358.

[7]. Han, H., et al., *Matching Composite Sketches to Face Photos: A Component-Based Approach.* IEEE Transactions on Information Forensics and Security, 2013. **8**(1): p. 191-204.

[8]. McQuiston-Surrett, D., L. Topp, and R. Malpass, *Use of facial composite systems in US law enforcement agencies.* Psychology, Crime & Law, 2006. **12**(5): p. 505-517.

[9]. Beham, M.P. and S.M. Mansoor Roomi, *A REVIEW OF FACE RECOGNITION METHODS.* International Journal of Pattern Recognition & Artificial Intelligence, 2013. **27**(4): p. 1-35.

[10]. Vinodini, R. and M. Karnan, *A SURVEY ON FACE RECOGNITION.* International Journal of Engineering Science and Technology, 2014. **6**(2): p. 45-48.

[11]. Li, S.Z. and A.K. Jain, *Handbook of face recognition*. 2011, New York; London: Springer.

[12]. Todd, J., *Digital image processing (second edition)*. 1988, Elsevier Ltd. p. 70-71.

[13]. http://www.wikipedia.com.

[14]. Shih, F.Y., *Image processing and pattern recognition: fundamentals and techniques*. 2010, Piscataway, NJ; Hoboken, N.J: IEEE Press.

[15]. Lu, J., K.N. Plataniotis, and A.N. Venetsanopoulos, *Face recognition using kernel direct discriminant analysis algorithms.* IEEE Transactions on Neural Networks, 2003. **14**(1): p. 117-126.

[16]. Kituyi, M., *Overview.* Least Developed Countries Report, 2013: p. I(13).

[17]. Ramchandra, A. and R. Kumar, *Overview Of Face Recognition System Challenges.*

[18]. Richa, J.K.J., *Face Recognition System–A Survey.*

[19]. Lajevardi, S., *Structural similarity classifier for facial expression recognition.* Signal, Image and Video Processing, 2014. **8**(6): p. 1103-1110.

[20]. Pantic, M. and I. Patras, *Dynamics of facial expression: recognition of facial actions and their temporal segments from face profile image sequences.* Systems, Man, and

Cybernetics, Part B: Cybernetics, IEEE Transactions on, 2006. **36**(2): p. 433-449.
[21]. Vincent, O. and O. Folorunso. *A descriptive algorithm for sobel image edge detection*.
[22]. Solomon, C. and T. Breckon, *Fundamentals of digital image processing: a practical approach with examples in Matlab*. 2011, Chichester: Wiley-Blackwell.
[23]. Jain, A.K., *Fundamentals of digital image processing*. 1989, Englewood Cliffs, NJ: Prentice Hall.
[24]. Prewitt, J.M., *Object enhancement and extraction.* Picture processing and Psychopictorics, 1970. **10**(1): p. 15-19.
[25]. Canny, J., *A computational approach to edge detection.* Pattern Analysis and Machine Intelligence, IEEE Transactions on, 1986(6): p. 679-698.
[26]. Bao, P., D. Zhang, and X. Wu, *Canny edge detection enhancement by scale multiplication.* Pattern Analysis and Machine Intelligence, IEEE Transactions on, 2005. **27**(9): p. 1485-1490.
[27]. Nercessian, S.C., K.A. Panetta, and S.S. Agaian, *Multiscale image fusion using an adaptive similarity-based sensor weighting scheme and human visual system-inspired contrast measure.* Journal of Electronic Imaging, 2012. **21**(2): p. 021112-1-021112-13.
[28]. Wharton, E.J., K.A. Panetta, and S.S. Agaian. *Human visual-system-based image enhancement*. 2007.
[29]. Agaian, S.S. *Visual morphology*. in *Electronic Imaging'99*. 1999. International Society for Optics and Photonics.
[30]. Panetta, K., et al., *Nonlinear unsharp masking for mammogram enhancement.* Information Technology in Biomedicine, IEEE Transactions on, 2011. **15**(6): p. 918-928.
[31]. Panetta, K., et al., *Parameterized logarithmic framework for image enhancement.* Systems, Man, and Cybernetics, Part B: Cybernetics, IEEE Transactions on, 2011. **41**(2): p. 460-473.
[32]. Lu, L., et al. *Comparative study of histogram equalization algorithms for image enhancement*. in *SPIE Defense, Security, and Sensing*. 2010. International Society for Optics and Photonics.
[33]. Nercessian, S., E. Tufts University. Department of, and E. Computer, *Human visual system-based multi-scale tools with biomedical and security applications*. 2012.
[34]. Kundu, M.K. and S.K. Pal, *Thresholding for edge detection using human psychovisual phenomena.* Pattern Recognition Letters, 1986. **4**(6): p. 433-441.
[35]. Hall, E., *Computer image processing and recognition*. 1979: Elsevier.
[36]. Zuidema, P., J.J. Koenderink, and M.A. Bouman, *A mechanistic approach to threshold behavior of the visual system.* Systems, Man and Cybernetics, IEEE Transactions on, 1983(5): p. 923-934.
[37]. Buchsbaum, G., *An analytical derivation of visual nonlinearity.* Biomedical Engineering, IEEE Transactions on, 1980(5): p. 237-242.
[38]. Senthilkumaran, N. and R. Rajesh, *Edge detection techniques for image segmentation–a survey of soft computing approaches.* International journal of recent trends in engineering,

2009. **1**(2).

[39]. Pentland, A., B. Moghaddam, and T. Starner. *View-based and modular eigenspaces for face recognition*. in *Computer Vision and Pattern Recognition, 1994. Proceedings CVPR'94., 1994 IEEE Computer Society Conference on*. 1994. IEEE.

[40]. Panetta, K.A., et al., *Human Visual System-Based Image Enhancement and Logarithmic Contrast Measure.* IEEE Transactions on Systems, Man, and Cybernetics, Part B (Cybernetics), 2008. **38**(1): p. 174-188.

[41]. Zhou, Y., et al. *Human visual system based mammogram enhancement and analysis*. IEEE.

[42]. Mandal, D., E. Tufts University. Department of, and E. Computer, *Human visual system based object detection and recognition and introduction of logarithmic local binary patterns for face recognition*. 2012.

[43]. Panetta, K., et al., *Nonreference Medical Image Edge Map Measure.* International Journal of Biomedical Imaging, 2014. **2014**: p. 1-8.

[44]. Hadid, A., M. Pietikainen, and T. Ahonen. *A discriminative feature space for detecting and recognizing faces*. in *Computer Vision and Pattern Recognition, 2004. CVPR 2004. Proceedings of the 2004 IEEE Computer Society Conference on*. IEEE.

[45]. Turk, M. and A. Pentland, *Eigenfaces for recognition.* Journal of cognitive neuroscience, 1991. **3**(1): p. 71-86.

[46]. Belhumeur, P.N., J.P. Hespanha, and D. Kriegman, *Eigenfaces vs. fisherfaces: Recognition using class specific linear projection.* Pattern Analysis and Machine Intelligence, IEEE Transactions on, 1997. **19**(7): p. 711-720.

[47]. Bartlett, M.S., J.R. Movellan, and T.J. Sejnowski, *Face recognition by independent component analysis.* Neural Networks, IEEE Transactions on, 2002. **13**(6): p. 1450-1464.

[48]. Gabor, D., *Theory of communication. Part 1: The analysis of information.* Journal of the Institution of Electrical Engineers-Part III: Radio and Communication Engineering, 1946. **93**(26): p. 429-441.

[49]. Wiskott, L., et al., *Face recognition by elastic bunch graph matching.* Pattern Analysis and Machine Intelligence, IEEE Transactions on, 1997. **19**(7): p. 775-779.

[50]. Lyons, M.J., J. Budynek, and S. Akamatsu, *Automatic classification of single facial images.* IEEE Transactions on Pattern Analysis and Machine Intelligence, 1999. **21**(12): p. 1357-1362.

[51]. Ojala, T., M. Pietikainen, and T. Maenpaa, *Multiresolution gray-scale and rotation invariant texture classification with local binary patterns.* Pattern Analysis and Machine Intelligence, IEEE Transactions on, 2002. **24**(7): p. 971-987.

[52]. Ahonen, T., A. Hadid, and M. Pietikainen, *Face description with local binary patterns: Application to face recognition.* Pattern Analysis and Machine Intelligence, IEEE Transactions on, 2006. **28**(12): p. 2037-2041.

[53]. Shan, C., S. Gong, and P.W. McOwan, *Facial expression recognition based on local binary patterns: A comprehensive study.* Image and Vision Computing, 2009. **27**(6): p.

803-816.
[54]. Jin, H., et al. *Face detection using improved LBP under bayesian framework*. in *Multi-Agent Security and Survivability, 2004 IEEE First Symposium on*. 2004. IEEE.
[55]. Zhang, L., et al., *Face detection based on multi-block lbp representation*, in *Advances in biometrics*. 2007, Springer. p. 11-18.
[56]. Zhang, H. and D. Zhao, *Spatial histogram features for face detection in color images*, in *Advances in Multimedia Information Processing-PCM 2004*. 2005, Springer. p. 377-384.
[57]. Chan, C.-H., J. Kittler, and K. Messer, *Multi-scale local binary pattern histograms for face recognition*. 2007: Springer.
[58]. Tan, X. and B. Triggs, *Enhanced local texture feature sets for face recognition under difficult lighting conditions.* Image Processing, IEEE Transactions on, 2010. **19**(6): p. 1635-1650.
[59]. Liao, S. and A.C. Chung, *Face recognition by using elongated local binary patterns with average maximum distance gradient magnitude*, in *Computer Vision–ACCV 2007*. 2007, Springer. p. 672-679.
[60]. Zhang, W., et al. *Multi-resolution histograms of local variation patterns (MHLVP) for robust face recognition*. in *Audio-and Video-Based Biometric Person Authentication*. 2005. Springer.
[61]. Li, S.Z., et al., *Learning to fuse 3D+ 2D based face recognition at both feature and decision levels*, in *Analysis and Modelling of Faces and Gestures*. 2005, Springer. p. 44-54.
[62]. Zhao, J., et al. *LBP discriminant analysis for face verification*. in *Computer Vision and Pattern Recognition-Workshops, 2005. CVPR Workshops. IEEE Computer Society Conference on*. 2005. IEEE.
[63]. Feng, X., A. Hadid, and M. Pietikäinen, *A coarse-to-fine classification scheme for facial expression recognition*, in *Image Analysis and Recognition*. 2004, Springer. p. 668-675.
[64]. Liao, S., et al. *Facial expression recognition using advanced local binary patterns, tsallis entropies and global appearance features*. in *Image Processing, 2006 IEEE International Conference on*. 2006. IEEE.
[65]. Zhao, G. and M. Pietikainen. *Experiments with facial expression recognition using spatiotemporal local binary patterns*. in *Multimedia and Expo, 2007 IEEE International Conference on*. 2007. IEEE.
[66]. Gritti, T., et al. *Local features based facial expression recognition with face registration errors*. in *Automatic Face & Gesture Recognition, 2008. FG'08. 8th IEEE International Conference on*. 2008. IEEE.
[67]. Sun, N., et al., *Gender classification based on boosting local binary pattern*, in *Advances in Neural Networks-ISNN 2006*. 2006, Springer. p. 194-201.
[68]. Yang, Z. and H. Ai, *Demographic classification with local binary patterns*, in *Advances in Biometrics*. 2007, Springer. p. 464-473.
[69]. Gao, X., et al., *Standardization of face image sample quality*, in *Advances in Biometrics*.

2007, Springer. p. 242-251.
[70]. Ma, B., et al. *Robust head pose estimation using LGBP*. in *Pattern Recognition, 2006. ICPR 2006. 18th International Conference on*. 2006. IEEE.
[71]. Ojala, T., M. Pietikäinen, and D. Harwood, *A comparative study of texture measures with classification based on featured distributions.* Pattern recognition, 1996. **29**(1): p. 51-59.
[72]. Ojala, T., M. Pietikainen, and D. Harwood. *Performance evaluation of texture measures with classification based on Kullback discrimination of distributions*. in *Pattern Recognition, 1994. Vol. 1-Conference A: Computer Vision & Image Processing., Proceedings of the 12th IAPR International Conference on*. 1994.
[73]. He, D.-C. and L. Wang. *Texture unit, texture spectrum and texture analysis*. in *IEEE Transactions on Geoscience and Remote Sensing*. 1989.
[74]. Pietikäinen, M., et al., *Computer vision using local binary patterns*. Vol. 40. 2011: Springer Science & Business Media.
[75]. Xiangsheng, H., S.Z. Li, and W. Yangsheng. *Shape localization based on statistical method using extended local binary pattern*. in *Multi-Agent Security and Survivability, 2004 IEEE First Symposium on*. 2004.
[76]. Huang, D., Y. Wang, and Y. Wang, *A robust method for near infrared face recognition based on extended local binary pattern*, in *Advances in Visual Computing*. 2007, Springer. p. 437-446.
[77]. Pham-Ngoc, P.-T. and K.-H. Jo. *Multi-face detection system in video sequence*. in *Strategic Technology, The 1st International Forum on*. 2006. IEEE.
[78]. Yang, H. and Y. Wang. *A LBP-based face recognition method with hamming distance constraint*. in *Image and Graphics, 2007. ICIG 2007. Fourth International Conference on*. 2007. IEEE.
[79]. Zhao, G. and M. Pietikainen, *Dynamic texture recognition using local binary patterns with an application to facial expressions.* Pattern Analysis and Machine Intelligence, IEEE Transactions on, 2007. **29**(6): p. 915-928.
[80]. Fu, X. and W. Wei. *Centralized binary patterns embedded with image Euclidean distance for facial expression recognition*. in *Natural Computation, 2008. ICNC'08. Fourth International Conference on*. 2008. IEEE.
[81]. Mandal, D., K. Panetta, and S. Agaian. *Face recognition based on logarithmic local binary patterns*. in *IS&T/SPIE Electronic Imaging*. 2013. International Society for Optics and Photonics.
[82]. Harandi, M.T., M.N. Ahmadabadi, and B.N. Araabi. *A hybrid model for face recognition using facial components*. in *Signal Processing and Its Applications, 2007. ISSPA 2007. 9th International Symposium on*. 2007. IEEE.
[83]. Sadr ô, J., I. Jarudi, and P. Sinha ô, *The role of eyebrows in face recognition.* Perception, 2003. **32**(3): p. 285-293.
[84]. Zhao, W., et al., *Face recognition: A literature survey*. Acm Computing Surveys (CSUR), 2003. **35**(4): p. 399-458.

[85]. Furl, N., P.J. Phillips, and A.J. O'Toole, *Face recognition algorithms and the other-race effect: computational mechanisms for a developmental contact hypothesis.* Cognitive Science, 2002. **26**(6): p. 797-815.
[86]. Diener-West, M., *Use of the Chi-Square Statistic.* 2008.
[87]. *http://www.face-rec.org/databases/*.
[88]. Zhang, G., et al., *Boosting local binary pattern (LBP)-based face recognition*, in *Advances in biometric person authentication*. 2005, Springer. p. 179-186.
[89]. Jolliffe, I., *Principal component analysis*. 2002: Wiley Online Library.
[90]. Scholkopft, B. and K.-R. Mullert. *Fisher discriminant analysis with kernels*. in *Proceedings of the 1999 IEEE Signal Processing Society Workshop Neural Networks for Signal Processing IX, Madison, WI, USA*. 1999.
[91]. Liu, C. and H. Wechsler, *Gabor feature based classification using the enhanced fisher linear discriminant model for face recognition.* Image processing, IEEE Transactions on, 2002. **11**(4): p. 467-476.
[92]. Cover, T. and P. Hart, *Nearest neighbor pattern classification.* Information Theory, IEEE Transactions on, 1967. **13**(1): p. 21-27.
[93]. Krizhevsky, A., I. Sutskever, and G.E. Hinton. *Imagenet classification with deep convolutional neural networks*. in *Advances in neural information processing systems*. 2012.
[94]. Li, S.Z. and J. Lu, *Face recognition using the nearest feature line method.* Neural Networks, IEEE Transactions on, 1999. **10**(2): p. 439-443.
[95]. Williams, C.K. and D. Barber, *Bayesian classification with Gaussian processes.* Pattern Analysis and Machine Intelligence, IEEE Transactions on, 1998. **20**(12): p. 1342-1351.
[96]. Nercessian, S.C., K.A. Panetta, and S.S. Agaian, *Multiresolution Decomposition Schemes Using the Parameterized Logarithmic Image Processing Model with Application to Image Fusion.* EURASIP Journal on Advances in Signal Processing, 2011. **2011**(1): p. 1-17.
[97]. Panetta, K., et al., *Parameterized Logarithmic Framework for Image Enhancement.* IEEE Transactions on Systems, Man, and Cybernetics, Part B (Cybernetics), 2011. **42**(2): p. 460-473.
[98]. Ahonen, T., A. Hadid, and M. Pietikäinen, *Face recognition with local binary patterns*, in *Computer vision-eccv 2004*. 2004, Springer. p. 469-481.
[99]. *http://www.imdb.com/*.
[100]. Houck, M.M., *Forensic Art and Illustration*. 2001, Forensic Science Society (UK). p. 290.
[101]. Ireland, C., et al., *An evaluation of US systems for facial composite production.* Ergonomics, 2007. **50**(12): p. 1987-1998.
[102]. http://www.askaforensicartist.com/composite-sketch-leads-to-arrest-in-virginia-highland-robbery/.

[103]. http://www.woodtv.com/dpp/news/local/grand_rapids/Sketch-leads-to-mans-assault-arrest#.
[104]. http://www.askaforensicartist.com/sketch-by-texas-rangers-forensic-artist-leads-to-id/.
[105]. http://www.facesid.com/mediacenter_frontline_stories.html.
[106]. http://captured.sketchcop.com/2011sketchcopcaptured_010.htm.
[107]. http://captured.sketchcop.com/2011sketchcopcaptured_002.htm.
[108]. Yuen, P.C., et al., *Human Face Image Searching System Using Sketches.* IEEE Transactions on Systems, Man, and Cybernetics - Part A: Systems and Humans, 2007. **37**(4): p. 493-504.
[109]. *https://secure.missingkids.org/donate/cawlanding.*